© 2015. Published by The Company of Biologists Ltd | Journal of Cell Science (2015) 128, 4196-4209 doi:10.1242/jcs.174441

RESEARCH ARTICLE

NRIP is newly identified as a Z-disc protein, activating calmodulin signaling for skeletal muscle contraction and regeneration

Hsin-Hsiung Chen[1], Wen-Pin Chen[2], Wan-Lun Yan[1], Yuan-Chun Huang[1], Szu-Wei Chang[1], Wen-Mei Fu[2], Ming-Jai Su[2], I-Shing Yu[3], Tzung-Chieh Tsai[4], Yu-Ting Yan[5], Yeou-Ping Tsao[6] and Show-Li Chen[1,*]

ABSTRACT

Nuclear receptor interaction protein (NRIP, also known as DCAF6 and IQWD1) is a Ca^{2+}-dependent calmodulin-binding protein. In this study, we newly identify NRIP as a Z-disc protein in skeletal muscle. NRIP-knockout mice were generated and found to have reduced muscle strength, susceptibility to fatigue and impaired adaptive exercise performance. The mechanisms of NRIP-regulated muscle contraction depend on NRIP being downstream of Ca^{2+} signaling, where it stimulates activation of both 'calcineurin-nuclear factor of activated T-cells, cytoplasmic 1' (CaN-NFATc1; also known as NFATC1) and calmodulin-dependent protein kinase II (CaMKII) through interaction with calmodulin (CaM), resulting in the induction of mitochondrial activity and the expression of genes encoding the slow class of myosin, and in the regulation of Ca^{2+} homeostasis through the internal Ca^{2+} stores of the sarcoplasmic reticulum. Moreover, NRIP-knockout mice have a delayed regenerative capacity. The amount of NRIP can be enhanced after muscle injury and is responsible for muscle regeneration, which is associated with the increased expression of myogenin, desmin and embryonic myosin heavy chain during myogenesis, as well as for myotube formation. In conclusion, NRIP is a novel Z-disc protein that is important for skeletal muscle strength and regenerative capacity.

KEY WORDS: NRIP, Z-disc, CaM, Muscle contraction, Regeneration

INTRODUCTION

The nuclear receptor interaction protein (NRIP) (also known as DCAF6 and IQWD1) is an androgen receptor (AR)-interacting protein (Tsai et al., 2005). In addition, NRIP is targeted by androgens and can stabilize the AR protein (Chen et al., 2008). NRIP comprises 860 amino acids and contains seven WD-40 repeats [40 amino acids terminating with a tryptophan and aspartic acid (W-D) dipeptide] and one IQ motif (Chang et al., 2011; Tsai et al., 2005). The IQ motif has been reported to be an interaction domain of proteins containing EF-hand motifs (Bähler and Rhoads, 2002) and, recently, NRIP has also been found to interact with calmodulin (CaM) in the presence of Ca^{2+} (Chang et al., 2011). In terms of diseases that are associated with NRIP, from genetic studies, genetic variations in NRIP genome location [NRIP in Chr1q24.2; reference sequence NC_000001.10 (167905797.. 168045081)] are associated with diseases such as cardiovascular disease, osteoporosis and schizophrenia (Cheung et al., 2009; Ehret et al., 2009; Shi et al., 2011). Hence, the involvement of the interaction of CaM with NRIP in disease should be interesting to explore.

CaM, together with Ca^{2+}, can activate calcineurin (CaN) and calmodulin kinases (CaMKs) (Bähler and Rhoads, 2002). When activated, CaN dephosphorylates transcription factors of the nuclear factor of activated T-cells (NFAT) family, leading to their nuclear translocation (Calabria et al., 2009), and activates the Ca^{2+}-dependent gene expression program (Harridge, 2007). The activation of CaN and NFAT specifically induces a muscle-fiber-type switch towards a slow-twitch and oxidative phenotype, allowing for sustained and fatigue-resistant muscle activity (Chin et al., 1998). The intracellular Ca^{2+} concentration is significantly higher in slow muscle fibers than it is in fast fibers (Harridge, 2007), and Ca^{2+} is the key factor for muscle contraction and relaxation (Lanner et al., 2010; Treves et al., 2008). Muscle contraction occurs when the muscles receive signals from motor neurons and produce an action potential that travels along the sarcolemma and voltage-gated Ca^{2+} channel in the T-tubule (dihydropyridine receptor) to depolarize the membrane, causing Ca^{2+} release from the *sarcoplasmic reticulum* (SR) through the ryanodine receptor (RyR) (Treves et al., 2008). Muscle relaxation occurs with the re-uptake of cytoplasmic Ca^{2+} into the SR through the SR Ca^{2+}-ATPases (SERCAs) of the Ca^{2+} pump, which stores SR Ca^{2+} at constant levels for the next round of contraction (Lanner et al., 2010). Thus, Ca^{2+} homeostasis is important for muscle contraction.

Compelling evidence shows that the CaN and CaMKII signaling pathways are involved in muscle repair and muscle regeneration (Demonbreun et al., 2010; McKinsey et al., 2000). Muscle degeneration and regeneration are tightly regulated in response to muscle injury. First, there is an inflammatory response in which phagocytes remove the damaged muscle fibers through phagocytosis. Then, satellite cells are activated and proliferate, and then transform into myoblasts. Sequentially, these myoblasts move to the site of the lesion to fuse with pre-existing myofibers or to form new myotubes for muscle regeneration (Borselli et al., 2010; Demonbreun et al., 2010; Mokalled et al., 2012; Shi and Garry, 2006).

Recently, in limb-girdle muscular dystrophy (LGMD) individuals, *NRIP* (*IQWD1*) RNA expression was found to be lower in dystrophy lesions than in counterpart normal tissues by examining the differential expression of the mRNA (Zhang et al., 2006). In this study, we generated NRIP-knockout mice and demonstrated that loss of NRIP leads to muscle dystrophy and delayed regeneration, with lower numbers of centralized nuclei and smaller myofiber size distribution, when compared with wild-type mice. In summary, NRIP regulates skeletal muscle strength and regenerative capacity.

[1]Graduate Institute of Microbiology, College of Medicine, National Taiwan University, Taipei 100, Taiwan. [2]Graduate Institute of Pharmacology, College of Medicine, National Taiwan University, Taipei 100, Taiwan. [3]Department of Clinical Laboratory Sciences and Medical Biotechnology, College of Medicine, National Taiwan University, Taipei 100, Taiwan. [4]Department of Microbiology, Immunology and Biopharmaceuticals, National Chiayi University, Chiayi 600-04, Taiwan. [5]Institute of Biomedical Sciences, Academia Sinica, Taipei 11529, Taiwan. [6]Department of Ophthalmology, Mackay Memorial Hospital, Taipei 104, Taiwan.

*Author for correspondence (showlic@ntu.edu.tw)

Received 14 May 2015; Accepted 25 September 2015

Journal of Cell Science

Journal of Cell Science (2015) 128, 4196-4209 doi:10.1242/jcs.174441

RESULTS

Decreased NRIP expression in aged mice

NRIP has been reported to activate CaN (Chang et al., 2011), which is located in the muscle sarcomere and has a role in muscle contraction (Frey and Olson, 2002; Frey et al., 2000). Therefore, we were interested in the role of NRIP in muscle function. First, NRIP protein expression was detected in the skeletal muscle, heart, lung, brain, thymus and testis of normal mice (Fig. S1A). In skeletal muscle, the majority of endogenous NRIP was expressed in the cytoplasm, and little in nucleus (Fig. 1A; Fig. S1B). NRIP colocalized with CaN at the Z-disc of the sarcomere, and myosin heavy chain (MyHC, pan-MyHC) was located at the center of the relaxed sarcomere and flanked with the dark doublet (A-band) that was connected to the Z-band (NRIP staining) (Fig. 1B). The results indicate that NRIP is a new Z-disc protein. Furthermore, the amount of NRIP protein was found to decline with advancing age, at 42 weeks, in the soleus and gastrocnemius in normal skeletal muscle (Fig. 1C). The rotarod test was used to measure the association of NRIP expression with muscle function. Older mice were more likely to fall off the apparatus and to run a shorter distance than younger mice (Fig. 1D), indicating that NRIP expression declines in older mice, as shown with weak rotarod activity. Thus, NRIP expression in skeletal muscle is age dependent.

Generation of NRIP-knockout mice

We generated conventional NRIP-knockout mice to investigate the role of NRIP *in vivo*. We designed the loxP-flanked exon 2 of the NRIP gene (Fig. 2A) for NRIP deletion. The deletion of NRIP exon 2 caused a frame shift mutation that resulted in premature termination. Southern blotting showed that the NRIP exon 2 had been deleted in homozygous knockout mice, as demonstrated with a band of 13 kb, compared to the size of the wild-type band of 16 kb (Fig. 2B). Using PCR analysis for genotyping, the NRIP knockout was confirmed by the loss of exon 2 (Fig. 2C). The NRIP protein was undetectable in lysates extracted from the gastrocnemius and soleus muscles of NRIP-knockout mice compared to that of wild-type littermates (Fig. 2D); the absence of NRIP protein was confirmed in muscle tissues using an immunohistochemical (IHC) assay (Fig. 2E). In addition, genotyping of newborn offspring from heterozygous matings showed that normal heterozygous and homozygous mutant mice were produced at the expected Mendelian ratios (data not shown). NRIP-knockout mice are viable and fertile.

NRIP-knockout mice have less muscle strength and endurance

To investigate the role of NRIP in muscle strength, muscle contractility was tested using the soleus, which contains a high number of slow fibers. To rule out the effect of neuromuscular transmission, the dissected soleus muscles were treated with the neuromuscular blocker d-tubocurarine (d-TC), an acetylcholine receptor antagonist (Martyn et al., 1992). A single twitch of muscle in male NRIP-knockout mice exhibited a significant reduction of force compared with that of wild-type littermates (Fig. 3A). Likewise, female NRIP-knockout mice produced less force than wild-type female littermates (Fig. 3B). Furthermore, the soleus muscles were assessed for fatigue resistance by repetitive stimulation to measure muscle endurance. The NRIP-knockout muscles were more susceptible to fatigue than their wild-type counterparts (Fig. 3C); similarly, the female NRIP-knockout mice showed less resistance to fatigue than wild-type females (Fig. 3D). Taken together, NRIP-knockout muscles in males and females have less muscle strength and endurance than their wild-type counterparts.

NRIP has been reported to have at least two functions – interaction with AR and stabilizing AR protein (Chen et al., 2008; Tsai et al., 2005), and Ca^{2+}-dependent CaM binding (Chang et al., 2011). Both AR and Ca^{2+}-dependent binding of CaM to NRIP have been reported to influence muscle strength (Bähler and Rhoads, 2002; MacLean et al., 2008). In terms of the effect of gender and AR on muscle force, the muscle force of the soleus in wild-type males did not differ significantly from that in their female counterparts (Fig. S2A), nor did NRIP-knockout males differ from NRIP-knockout females (Fig. S2B). However, the resistance of wild-type females to fatigue was greater than wild-type males (Fig. S2C), consistent with previous reports (MacLean et al., 2008; Ophoff et al., 2009); similarly, the resistance of NRIP-knockout females to fatigue was higher than NRIP-knockout males (Fig. S2D). In summary, the deprivation of NRIP causes a reduction of muscle force and endurance, regardless of gender; AR protein expression levels did not differ between male and female soleus muscles either (Fig. S2E). In addition, there did not appear to be any effect of knocking out NRIP on the protein levels of AR (Fig. S2F), indicating that NRIP cannot regulate AR protein expression in muscle. It seems that NRIP regulates muscle strength and endurance downstream of AR. In this study, to rule out AR and gender effects, the subsequent experiments were conducted on male mice to focus on the interaction between NRIP and Ca^{2+}-dependent CaM binding during muscle contraction.

We then determined whether NRIP could affect CaM protein expression. The expression of CaM protein in NRIP-knockout mice was unaltered, in comparison to that in wild-type mice (Fig. S2F). CaM can interact with CaN or CaMKII to activate phosphatase and kinase activity, respectively. Hence, we investigated whether the interaction of CaM with CaN or CaMKII could be influenced by the absence of NRIP. As shown in Fig. 3E, the amount of CaN and CaMKII was lower in knockout mice, following co-immunoprecipitation with CaM, than in wild-type mice. This indicates that NRIP can affect the binding affinity of CaM for CaN and CaMKII, but not the level of CaM protein.

NRIP-knockout mice have impaired adaptive exercise performance

The rotarod test was used to investigate muscle adaptation to the increased contraction activity. NRIP-knockout mice fell off the rotating cylinder of the rotarod much sooner, having run a shorter distance than wild-type littermates (Fig. 3F). In addition, a treadmill analysis was conducted by measuring the frequency of electrical stimulation by the electrical probe in the forced treadmill, which forced the mice to run when they stopped. NRIP-knockout mice had a higher number of electrical stimulations whilst running on the treadmill than did wild-type mice (Fig. 3G). Taken together, these data show that NRIP plays an important role in adaptive exercise performance.

NRIP affects muscle strength through CaN-NFATc1

NRIP can activate CaN (Chang et al., 2011). The activated CaN dephosphorylates NFATc1 and triggers the expression of a subset of genes, such as type-I slow myosin and myocyte-enriched calcineurin-interacting protein 1 (MCIP1; also known as RCAN1). Therefore, we hypothesized that the weak muscle strength of NRIP-knockout mice might result from decreased CaN activity through loss of Ca^{2+}-dependent CaM binding. Hence, dephosphorylated NFATc1 (active form) and phosphorylated NFATc1 (inactive form) were examined in isolated muscle

Journal of Cell Science (2015) 128, 4196-4209 doi:10.1242/jcs.174441

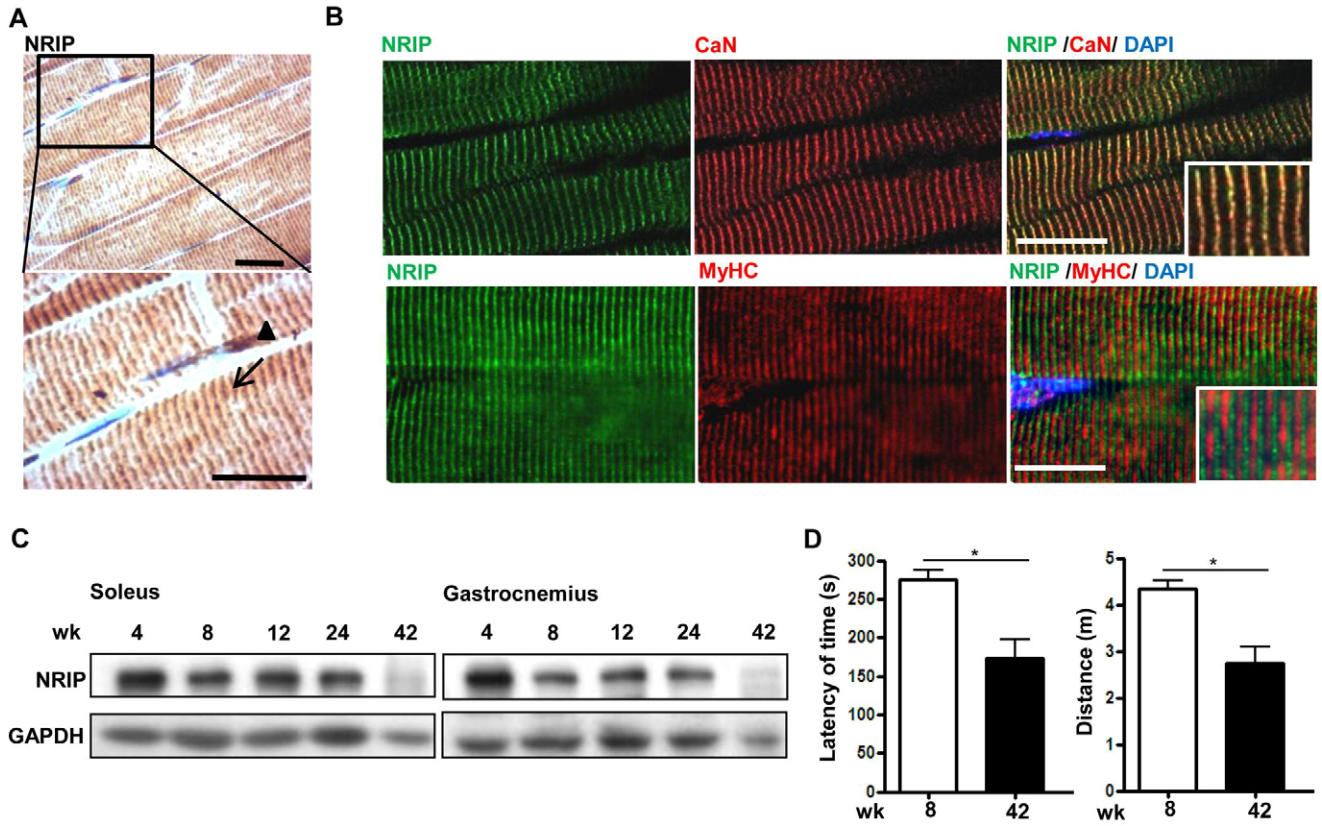

Fig. 1. NRIP expression in skeletal muscle is age dependent. (A) The sublocalization of NRIP protein in skeletal muscle tissues. The expression of NRIP was analyzed with immunohistochemistry analysis of longitudinal sections of diaphragms. Arrowhead, nucleus; arrow, cytoplasm. Scale bars: 50 µm. (B) NRIP colocalizes with calcineurin (CaN) in the Z-disk. The relaxed gastrocnemius muscles of wild-type mice were excised following perfusion with 0.5% lidocaine; and then analyzed with confocal microscopy. Green, NRIP (upper and lower panel); red upper, CaN; lower, MyHC (pan-MyHC); yellow, colocalization. Scale bars: 20 µm. (C) NRIP expression in the soleus and gastrocnemius at the ages indicated, detected by western blotting. Wk, week. (D) Rotarod assays of mice at ages 12 and 42 weeks. Mice were placed on a rod rotating and the time taken for them to fall was measured (left), and the distance was calculated as rod diameter×rotating speed×time on rod (right). n=6. Mean±s.e.m., n=6, *P<0.05 (Student's t-test).

tissues. The expression of dephosphorylated NFATc1 was reduced in both the soleus and gastrocnemius muscles of NRIP-knockout mice (Fig. 4A,B). To evaluate the effect of NRIP on CaN, we measured the mRNA levels of *MCIP1* (MCIP1 is used as a marker in the traditional CaN enzyme activity assays), slow (types I and IIa, also known as MYH10 and MYH9, respectively) and fast myosin (types IIx and IIb, also known as MYH1 and MYH4, respectively) using real-time quantitative (q)PCR (Bassel-Duby and Olson, 2006). The slow myosin (types I and IIa) and *MCIP1* mRNA levels were decreased significantly in the soleus and gastrocnemius muscles of NRIP-knockout mice when compared with those of wild-type mice (Fig. 4C,D), and these results were in accordance with the decreased levels of dephosphorylated NFATc1 in the knockout mice (Fig. 4A,B). Confirming the effect of NRIP on slow myosin protein expression, the amount of slow myosin (myosin heavy chain slow isoform) protein was reduced in NRIP-knockout mice compared to that in wild-type mice (Fig. 4E). The ratio of slow-myosin-positive myofibers to total myofibers, calculated using immunofluorescent antibody staining (Fig. 4F), was also significantly lower in the soleus muscles of NRIP-knockout mice than those of wild-type mice. Hence, NRIP has the ability to activate the CaN-NFATc1 pathway in skeletal muscle.

NRIP has an effect on mitochondrial activity

The biogenesis and function of mitochondria have been shown to affect muscle force. The peroxisome-proliferator-activated receptor γ coactivator 1α (PGC1-α; also known as PPARGC1A) is one of the key regulators of the oxidative metabolism of muscle, increasing mitochondrial biogenesis and augmenting the expression of enzymes in the electron transport system, such as cytochrome *c* oxidase (COX) and succinate dehydrogenase (SDH) (Garcia-Roves et al., 2006; Russell et al., 2014). Real-time PCR analysis revealed that PGC1-α expression was significantly decreased in skeletal muscle cells (C2C12) that had been infected with an adenovirus construct expressing a small hairpin (sh)RNA against NRIP (named Ad-shNRIP) to knockdown endogenous NRIP expression (Fig. 4G). Furthermore, histochemical staining revealed that the soleus muscle of NRIP-knockout mice contained fewer COX- and SDH-positive myofibers than those of wild-type mice (Fig. 4H,I). Taken together, these data suggest that the role of NRIP in regulating muscle force might be derived from the effect on mitochondrial activity.

NRIP stimulates phosphorylation of CaMKII

In addition to the activation of CaN-NFATc1, CaM also can trigger CaMKII activation (Bähler and Rhoads, 2002). Because NRIP is a CaM-binding protein (Chang et al., 2011), it has been suggested to activate phosphorylation of CaMKII. Exercise can stimulate CaMKII phosphorylation at residue Thr287 in skeletal muscle, and there is a strong correlation between CaMKII Thr287 phosphorylation and autonomous CaMKII activity (Bassel-Duby and Olson, 2006; Rose et al., 2006). Therefore, the amount of

Journal of Cell Science (2015) 128, 4196-4209 doi:10.1242/jcs.174441

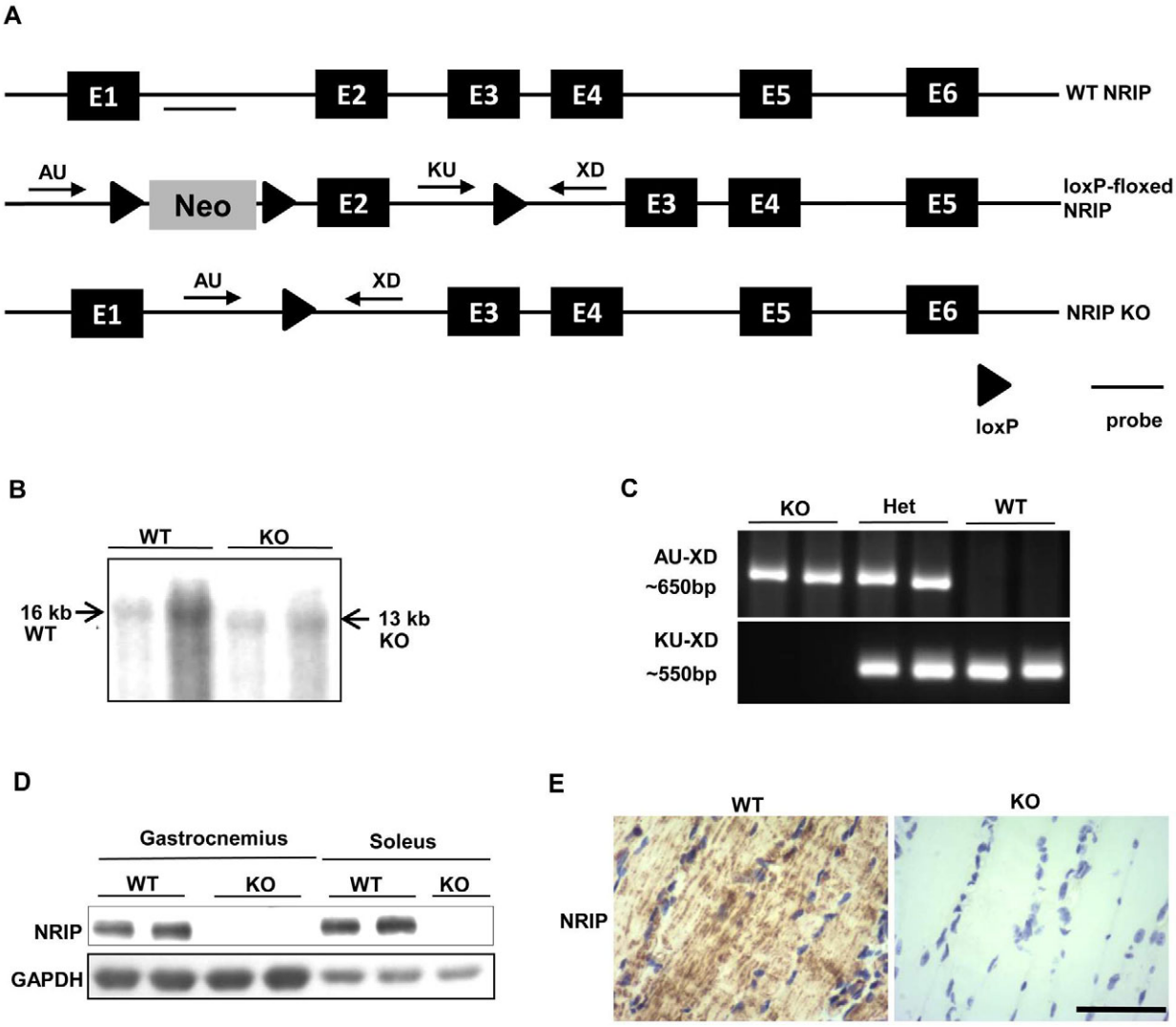

Fig. 2. Generation of NRIP-knockout mice. (A) Schematic illustration of the genomic structure of *NRIP*, loxP-floxed *NRIP* and NRIP-knockout. The loxP-floxed allele contains a neo cassette with two flanking loxP sequences in intron 1 and a loxP sequence in intron 2. NRIP exon (E)2 was deleted by using Cre recombinase. AU, XD and KU are primers. (B) Southern hybridization. The wild-type allele presents a band of 16 kb, and the NRIP-knockout allele presents a 13 kb band. *n*=2. (C) Genotyping by using PCR analysis. The locations of the probes, AU, XD and KU are shown in Panel A. The exon 2 and neo cassette was deleted by Cre recombinase; hence the designed KU sequences should be removed in the NRIP-knockout. The 650-bp band detected by AU–XD is a target product, but the large size of AU–XD in the wild-type (WT) containing intron 1 is not shown. The 550-bp band detected by KU–XD is a wild-type product. *n*=2. KO, knockout; Het, heterozygous. (D) Loss of mouse NRIP protein expression in the skeletal muscle tissues of knockout mice. The NRIP protein expression in the soleus and gastrocnemius was analyzed by western blotting. In the data represented above: gastrocnemius, WT (*n*=2), KO (*n*=2); soleus, WT (*n*=2), KO (*n*=1). (E) Immunohistochemistry analysis of NRIP expression. Sections of diaphragm muscle from each genotype were examined. Scale bar: 50 µm.

CaMKII produced in response to electrical stimulation (pacing), and its phosphorylation status, were determined. In response to pacing, phosphorylated CaMKII could be induced significantly in the muscles of wild-type mice (Fig. 5A, lane 2) but not those of knockout mice (lane 4). There was no significant difference between wild-type and knockout mice at rest (Fig. 5A, lanes 1 and 3). In summary, NRIP-knockout mice have impaired CaMKII signaling in response to electrical stimulation (pacing).

Activated CaMKII can cause phosphorylation of RyRs and open channels in the SR to release free Ca^{2+} (Rose et al., 2006). Furthermore, phosphorylated CaMKII can also enhance the activity of SERCAs to take up Ca^{2+}. Ca^{2+} release and uptake of SR through electrical stimulation are coupled with muscle excitation and contraction. We then measured the transient Ca^{2+} release from the SR into the cytoplasm through electrical stimulation at 1 Hz. The release of Ca^{2+} by each genotype was indicated by the fluorescence signal of Fura-2 (Fig. 5B, upper chart), the amplitude peak was lower in NRIP-knockout mice than that in wild-type mice (Fig. 5B, lower graph). Thus, NRIP-knockout mice showed a decline of transient Ca^{2+} release that could be the result of either RyR dysfunction or impaired Ca^{2+} reuptake into the SR (Gonzalez et al., 2007). We sought to differentiate the effect of NRIP on Ca^{2+} release from the SR and on the storage of Ca^{2+} in the SR. Caffeine, a RyR1 agonist, can stimulate RyR1 opening for maximal Ca^{2+} release from the SR into the cytosol. The amplitude of the caffeine-induced transient can be considered as the Ca^{2+} storage level of the SR. The Ca^{2+} released completely from the SR was measured after caffeine treatment without electrical stimulation; the amount of Ca^{2+} storage was lower in NRIP-knockout mice than in wild-type mice (Fig. 5C). Altogether, the Ca^{2+} storage in the SR is reduced in NRIP-deficient

Journal of Cell Science (2015) 128, 4196-4209 doi:10.1242/jcs.174441

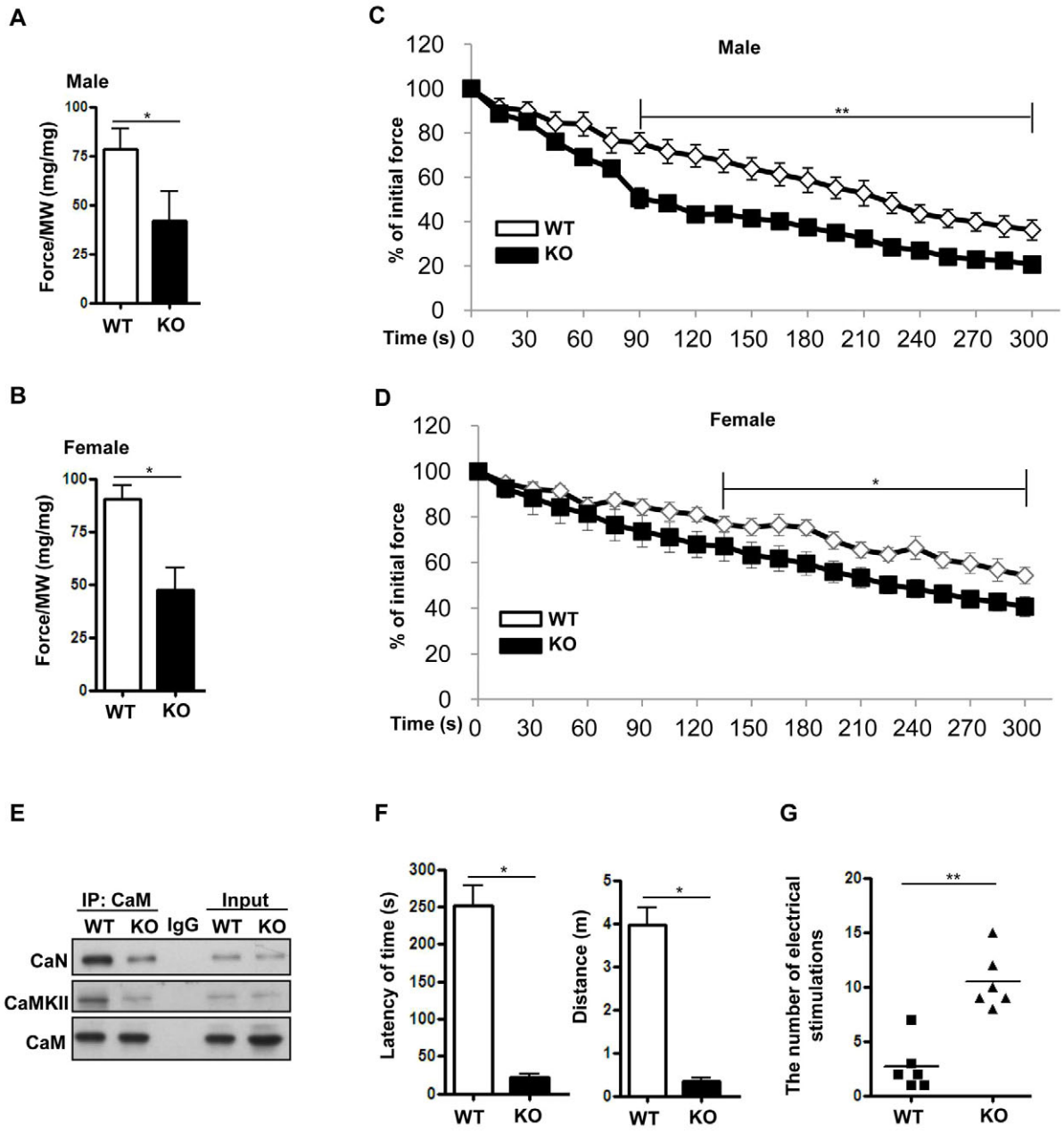

Fig. 3. NRIP-knockout mice lose muscle strength and endurance. (A) Isometric twitch force of soleus muscles in males. The isometric force was measured as described in Materials and Methods, and normalized with the corresponding muscle weight (MW). (B) Isometric force of female mice. (C) Fatigue-resistance assay of the soleus muscle in males. Fatigue was recorded by the decline of relative force to the initial force by repetitive stimulations at a given time. (D) Fatigue-resistance assay of females. (E) The decreased interaction affinity between CaM with CaN or CaMKII in NRIP-knockout mice. Equivalent amounts of protein lysate from the soleus muscles were immunoprecipitated (IP) using an antibody against CaM, and the samples were analyzed by western blotting with antibody against CaN or CaMKII. (F) Rotarod test. The time on the rotating rod before falling (left) and distance (right) are recorded the same as in Fig. 1D. (G) The treadmill test. *y*-axis, the number of electrical stimulations within 10 min was plotted for each mouse. All the data (A–G) are from six independent experiments for statistical analysis. KO, knockout; WT, wild type. Mean±s.e.m., n=6, *P<0.05, **P<0.01 (Student's t-test).

muscles, resulting in the disruption of Ca^{2+} release from the SR into the cytosol. Moreover, an immunofluorescence assay showed that the physical location of CaM with CaN (Fig. S3A) or CaMKII in the sarcomere in NRIP-knockout mice was comparable to that in wild-type mice (Fig. S3B). Western blot analysis of the Ca^{2+}-handling proteins revealed that the expression levels of RyR1, dihydropyridine receptor and SERCAs in NRIP-knockout mice were the same as in wild-type mice (Fig. S3C). Taken together, NRIP does not control the expression and structural location of Ca^{2+}-linked proteins. In addition, the triad structure of Ca^{2+}-release units was observed by using transmission electron microscopy in knockout mice, and the size of two junctional SR-adjacent T-tubules was significantly smaller than that in wild-type mice (Fig. 5D). The deficiency of NRIP resulted in a Ca^{2+}-release defect of the SR that might be attributable to the low Ca^{2+}-storage of the SR, leading to reduced muscle contractile strength and endurance. Taken together, NRIP regulates CaMKII phosphorylation and the balance of Ca^{2+} storage in the SR.

Journal of Cell Science (2015) 128, 4196-4209 doi:10.1242/jcs.174441

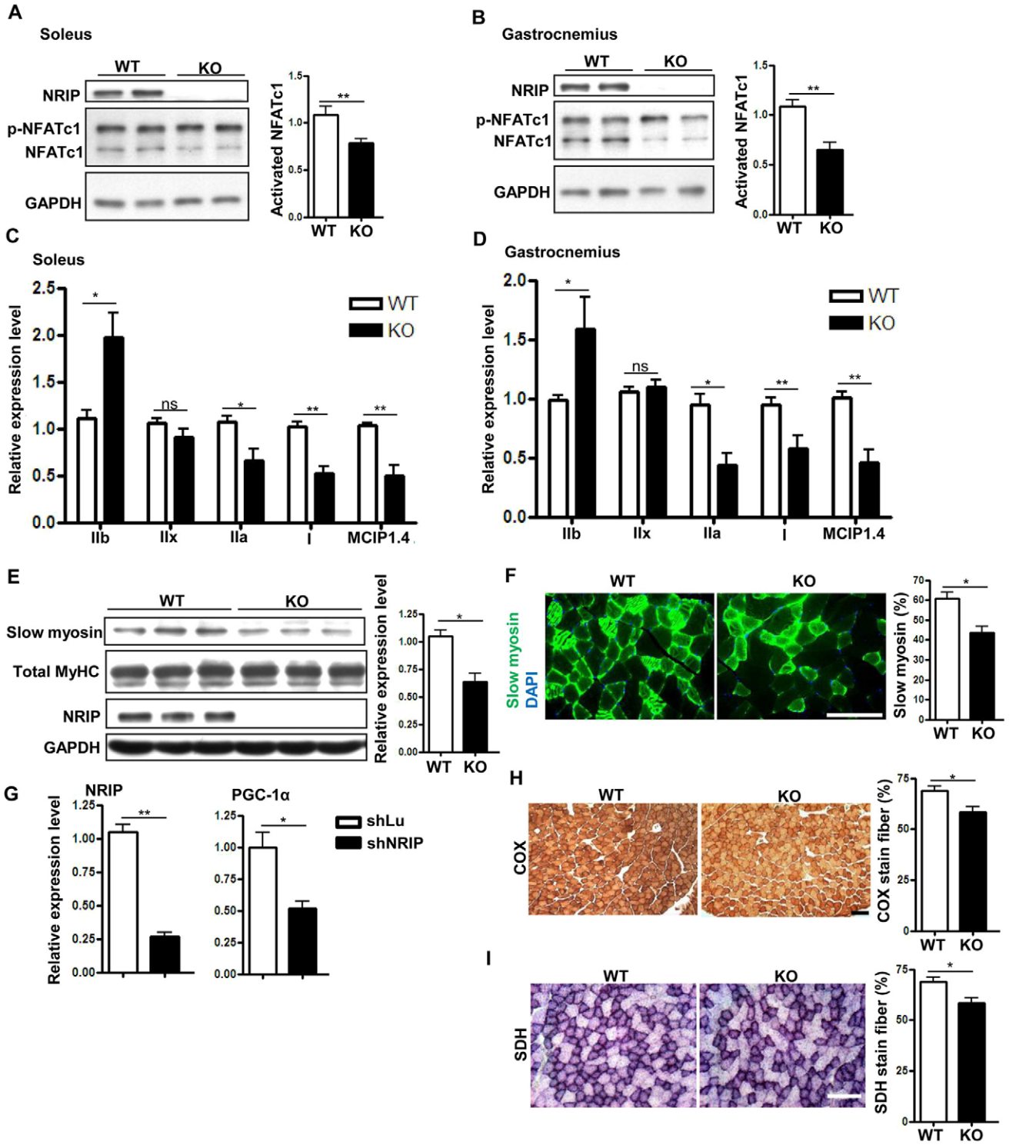

Fig. 4. NRIP activates the CaN–NFATc1 pathway. (A,B) NRIP-knockout mice have less activated NFATc1. NFATc1, activated NFATc1 (dephosphorylated); p-NFATc1, phosphorylated NFATc1. Left, a representative western blot, *n*=2. Right, quantification of the left panel. The activated NFATc1 was normalized to total NFATc1 (phosphorylated and unphosphorylated NFATc1) and set at 1 for the wild-type. (A) Soleus and (B) gastrocnemius. *n*=6. (C,D) NFATc1-target gene expression. The RNAs of fast myosins [MyHC IIb (*MYH4*), MyHC IIx (*MYH1*) and MyHC IIa (*MYH9*)], slow myosin [myosin I (*MYH7*)] and MCIP1.4 (an activated-NFATc1 reporter gene for positive control) were analyzed with RT-qPCR. (C) Soleus, *n*=6; (D) gastrocnemius, *n*=6. (E) Slow myosin (myosin heavy chain slow isoform) protein expression by western blotting. *n*=3. Left, western blot; right, quantification from the left panel. (F) Slow myosin expression by using an immunofluorescence assay. Cross sections of soleus tissues were stained with an antibody against slow myosin (myosin heavy chain slow isoform) and counterstained with DAPI to locate the nuclei. Left, one representative experiment; right, quantitation of slow myosin expression, *n*=6. Scale bar: 100 µm. (G) Quantification of the mRNA of PGC-1α by using RT-qPCR. NRIP expression in C2C12 cells was silenced through expression of an shRNA against NRIP (shNRIP); the expression of the transcripts was normalized to that of GAPDH. shLu, control shRNA against luciferase. *n*=3. (H) Representative images of soleus muscle cross sections with staining of COX (dark brown). Scale bar: 100 µm. (I) Staining of SDH (dark purple). All images were quantified by using Axiovision software. *n*=6. Scale bar: 100 µm. KO, knockout; ns, not significant; WT, wild type. Mean±s.e.m.; **P*<0.05, ***P*<0.01 by Student's *t*-test.

Journal of Cell Science (2015) 128, 4196-4209 doi:10.1242/jcs.174441

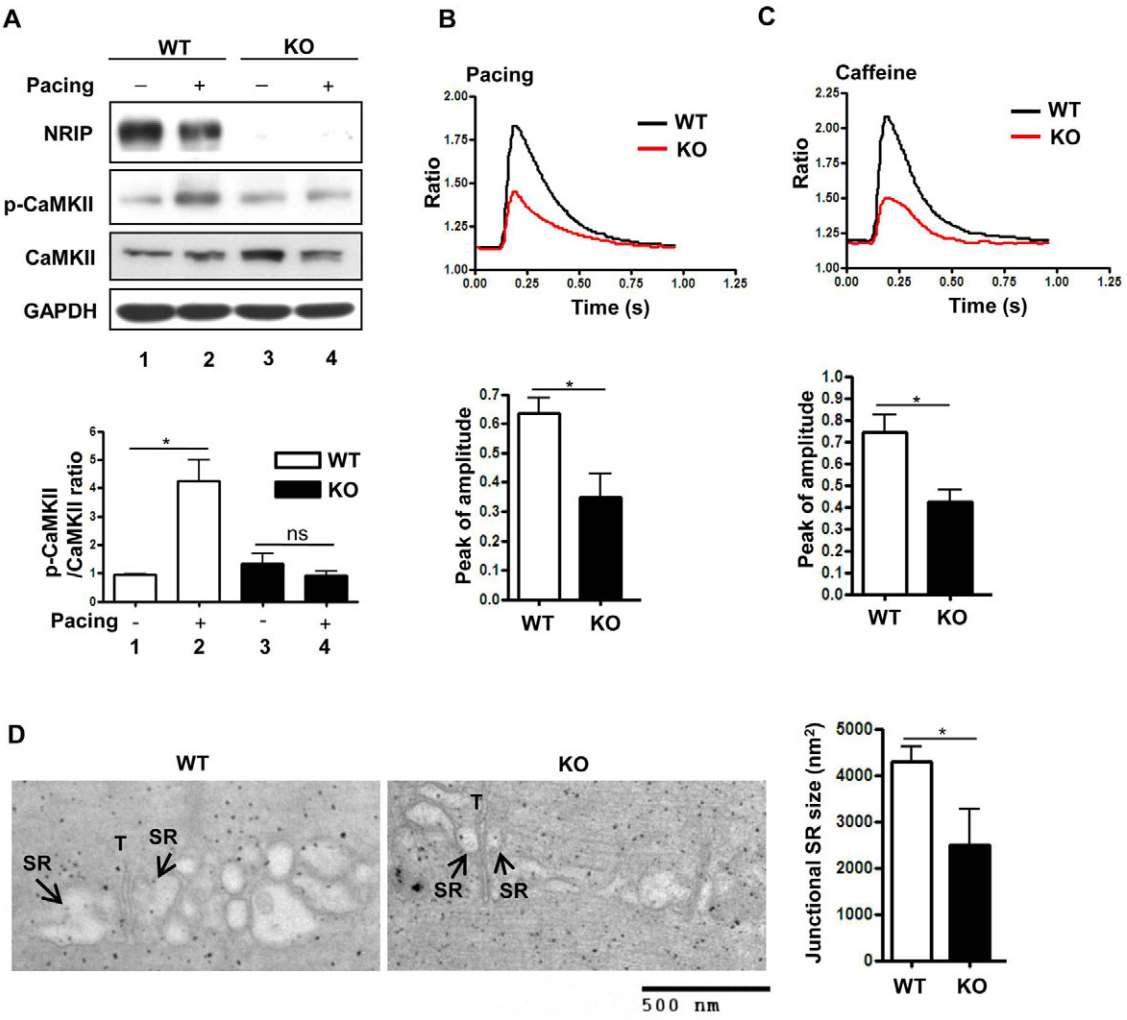

Fig. 5. NRIP mediates phosphorylation of CaMKII and the balance of Ca^{2+} storage in the SR. (A) The amount and phosphorylation status of CaMKII. Levels of CaMKII were measured in response to platinum wire electrodes (pacing). Upper panel, a representative western blot. Lower, quantification of the ratio of phosphorylated CaMKII to total CaMKII. *n*=3. (B) Ca^{2+} transient release. Upper panel, one representative tracing of Ca^{2+} flux stimulated by 1 Hz. Lower panel, the cumulative data of Ca^{2+}amplitudes from wild-type (*n*=10) and NRIP-knockout mice (*n*=9). (C) Complete Ca^{2+} release from the SR into the cytoplasm, induced by caffeine. Upper panel, a representative tracing of Ca^{2+} flux upon treatment with caffeine without electric stimulation. Lower panel, the cumulative data from wild-type (*n*=8) and knockout mice (*n*=12). (D) Transmission electron microscopy of the size of junctional SR. Left, image of the triad structure of Ca^{2+}-release units, including one T-tubule (T) and two junctional SR (arrows). Right, quantification of the junctional SR area of three samples from each genotype using ImageJ. KO, knockout; ns, not significant; WT, wild type. Mean±s.e.m.; **P*<0.05 (Student's *t*-test).

NRIP acts downstream of Ca^{2+} signaling to activate both CaN and CaMKII through interaction with CaM

Mouse myoblast C2C12 cells were used to investigate further the mechanisms of NRIP stimulation of CaN and CaMKII. C2C12 cells were infected with Ad-shNRIP and treated with a Ca^{2+} ionophore (A23187) that can trigger Ca^{2+}-mediated signaling, including CaN and CaMKII activation. The expression levels of activated NFATc1 and phosphorylated CaMKII decreased with the depletion of NRIP without A23187 (Fig. 6A, lane 2 compared to lane 1), and the activated NFATc1 and phosphorylated CaMKII increased when the cells were treated with A23187 alone (Fig. 6A, lane 3 compared to lane 1). When A23187 and Ad-shNRIP were combined, the loss of CaN and CaMKII activities could not be restored (Fig. 6A, lane 4 compared to lane 2). Additionally, the activated NFATc1 can be translocated into the nucleus and, when the cells were infected with Ad-shNRIP to reduce endogenous NRIP protein expression, we noted the elimination of nuclear NFATc1; instead, most NFATc1 remained in the cytosol. Similarly, A23187 could not rescue the activity of CaN (Fig. 6B). Taken together, the silencing of NRIP expression in cell culture supports the data from NRIP-knockout mice, indicating that the loss of NRIP causes a decrease of CaN-NATc1 activity and phosphorylation of CaMKII. When NRIP expression was forced by using recombinant adenovirus infection (with a construct named Ad-NRIP), the levels of activated NFATc1 and phosphorylated CaMKII increased (data not shown).

The IQ domain of NRIP is responsible for binding to CaM (Chang et al., 2011). To confirm that NRIP induces the activities of CaN and CaMKII through Ca^{2+}-dependent CaM binding, the forced expression of the truncated IQ domain of NRIP was induced by using another adenovirus (named Ad-NRIPΔIQ) with A23187. NRIPΔIQ did not activate NFATc1 and phosphorylated CaMKII owing to the loss of CaM binding (Fig. 6C, lanes 1 and 2) and A23187 could not restore these two activities (Fig. 6C, lanes 2 and 4). Furthermore, the slow myosin and *MCIP1* mRNA levels were significantly decreased through the deprivation of NRIP (Fig. 6D). This confirms further the decreased expression of slow myosin in NRIP-knockout mice *in vivo*

Journal of Cell Science (2015) 128, 4196-4209 doi:10.1242/jcs.174441

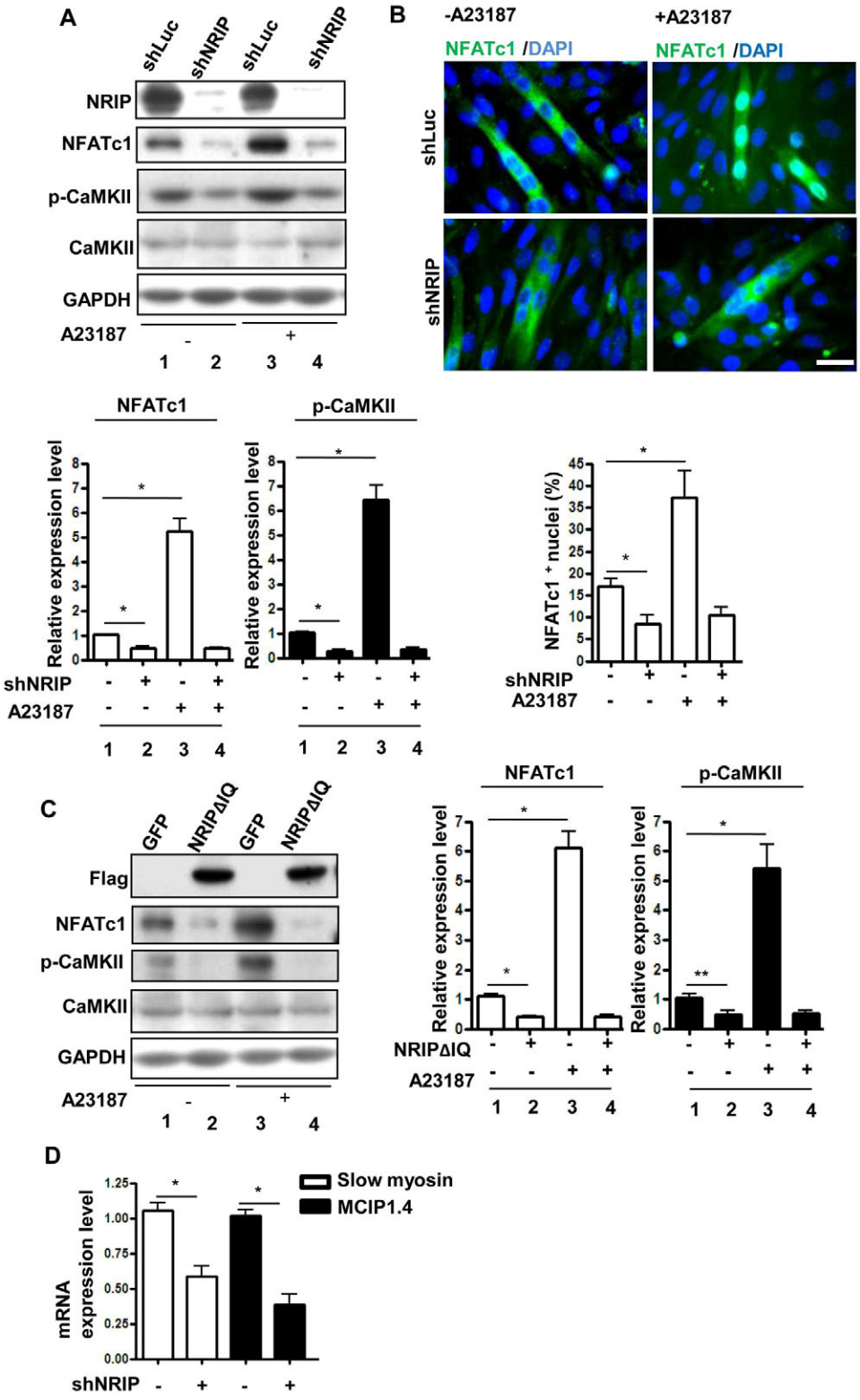

Fig. 6. NRIP acts downstream of Ca^{2+} signaling to activate both CaN and CaMKII through interaction with CaM. (A) Silencing NRIP decreases CaN and CaMKII activity in cells. C2C12 cells were infected with Ad-shNRIP or Ad-shLuc (multiplicity of infection=10) and incubated for 3 days and then treated with 1 µM A23187 for 24 h. Upper panel, one representative experiment. Lower, the relative expression levels of the activated NFATc1 (dephosphorylated) and phosphorylated (p-)CaMKII for each group compared to that of the control (shLuc without A23187, set as 1). *n*=3. (B) Subcellular location of NFATc1. Upper panel, a representative image of the immunofluorescence assay. NFATc1 (green), DAPI counter stain (blue). Lower panel, the percentage of the total number of nuclei that had NFATc1 localization. *n*=3. Scale bar: 50 µm. (C) The IQ domain of NRIP is responsible for CaM signaling. Cells were infected with Ad-NRIPΔIQ in the presence or absence of A23187, as described in panel A. Left, one representative experiment. Right, the relative levels of NFATc1 and phosphorylated CaMKII in each group compared those of the control without A23187 (set as 1). *n*=3. (D) RT-qPCR analysis of slow myosin and MCIP1.4 expression. C2C12 cells were infected with Ad-shNRIP and then shifted to differentiation medium for another 3 days. *n*=6. Mean±s.e.m.; **P*<0.05, ***P*<0.01 by Student's *t*-test.

(Fig. 4C,D). Altogether, NRIP acts downstream of Ca^{2+} signaling to activate both CaN and CaMKII, through interaction with CaM.

NRIP-knockout mice have delayed skeletal muscle regeneration

As mentioned above, NRIP can stimulate CaN-NFATc1 and CaMKII phosphorylation to trigger muscle excitation and contraction. Both CaN and CaMKII have been reported to be involved in muscle regeneration after muscle injury (Abraham and Shaw, 2006; Demonbreun et al., 2010). To investigate extensively the potential role of NRIP in muscle regeneration, wild-type and NRIP-knockout mice were injected with cardiotoxin (CTX) unilaterally into the tibialis anterior muscle, the contralateral muscle was injected with PBS as a control (Frey et al., 2008). NRIP-knockout mice did not exhibit apparent histological muscle defects under normal conditions (Fig. 7A, uninjured panel). The

Journal of Cell Science (2015) 128, 4196-4209 doi:10.1242/jcs.174441

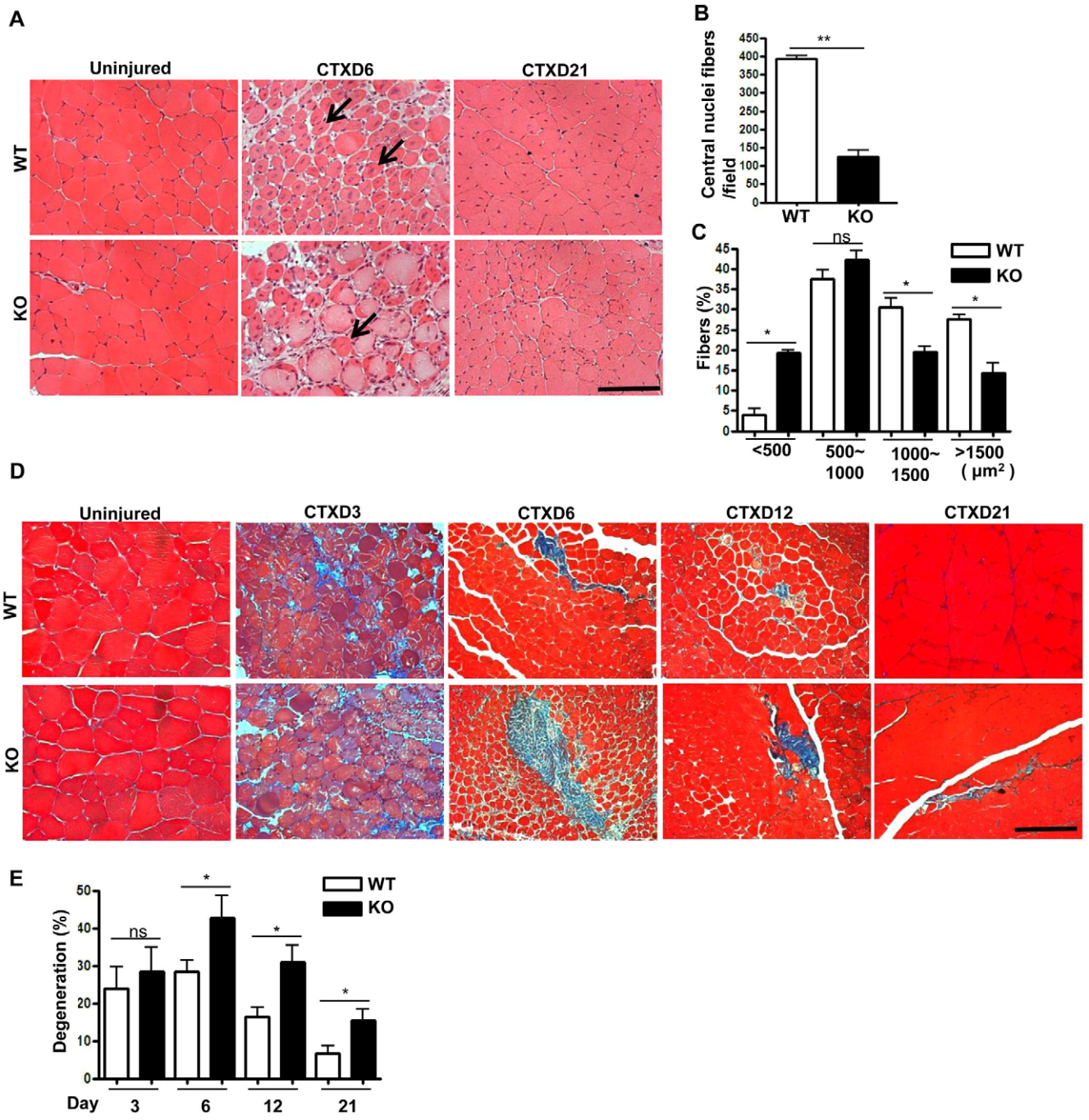

Fig. 7. NRIP-knockout mice have delayed skeletal muscle regeneration after CTX injury. (A) HE staining of cross-sections of tibialis anterior muscles from wild-type and NRIP-knockout mice at days 0, 6 and 21 after injury with CTX. Arrows, central nuclei; CTXD6 and CTXD21, 6 and 21 days after injury with CTX. Scale bar: 100 μm. (B) Quantification of centralized nuclei at day 6 post injury. *n*=6. (C) Quantification of fiber size at day 21 post injury. *n*=6. (D) Masson's trichrome staining of tibialis anterior muscles at day 0, 3, 6, 12 and 21 post injury. Scale bar: 100 μm. (E) Quantification of the degenerative proportion on the day indicated after muscle injury. *n*=6. The degenerated area was evaluated for fibrosis (blue staining) using the ImageJ program. The data in B,C,E were counted from a microscopic field (5×10^4 μm^2) after muscle injury. KO, knockout; ns, not significant; WT, wild type. Mean±s.e.m.; **P*<0.05, ***P*<0.01 (Student's *t*-test).

newly regenerated myofibers with centralized nuclei could be distinguished from pre-existing myofibers, in which the nuclei are positioned at the cell periphery (Mokalled et al., 2012). Six days after CTX injection, the newly formed myofibers had been filled in (Fig. 7A, CTXD6), and the number of centralized nuclei was significantly higher in wild-type than in knockout mice at day 6 post injury (Fig. 7B). At day 21 post injury, restored muscle architecture was seen in both wild-type and knockout mice. However, in terms of myofiber size and distribution at day 21 post injury, NRIP-knockout mice had a significantly higher frequency of small fiber size distribution than wild-type mice (Fig. 7C), indicating that NRIP-knockout mice have a delayed regeneration response. Masson's trichrome staining was used to reveal the accumulation of fibrosis by examining collagen deposition, a marker of degeneration in damaged muscles. NRIP-knockout mice did not display obvious fibrosis under normal conditions (Fig. 7D, uninjured panel). Three

Journal of Cell Science (2015) 128, 4196-4209 doi:10.1242/jcs.174441

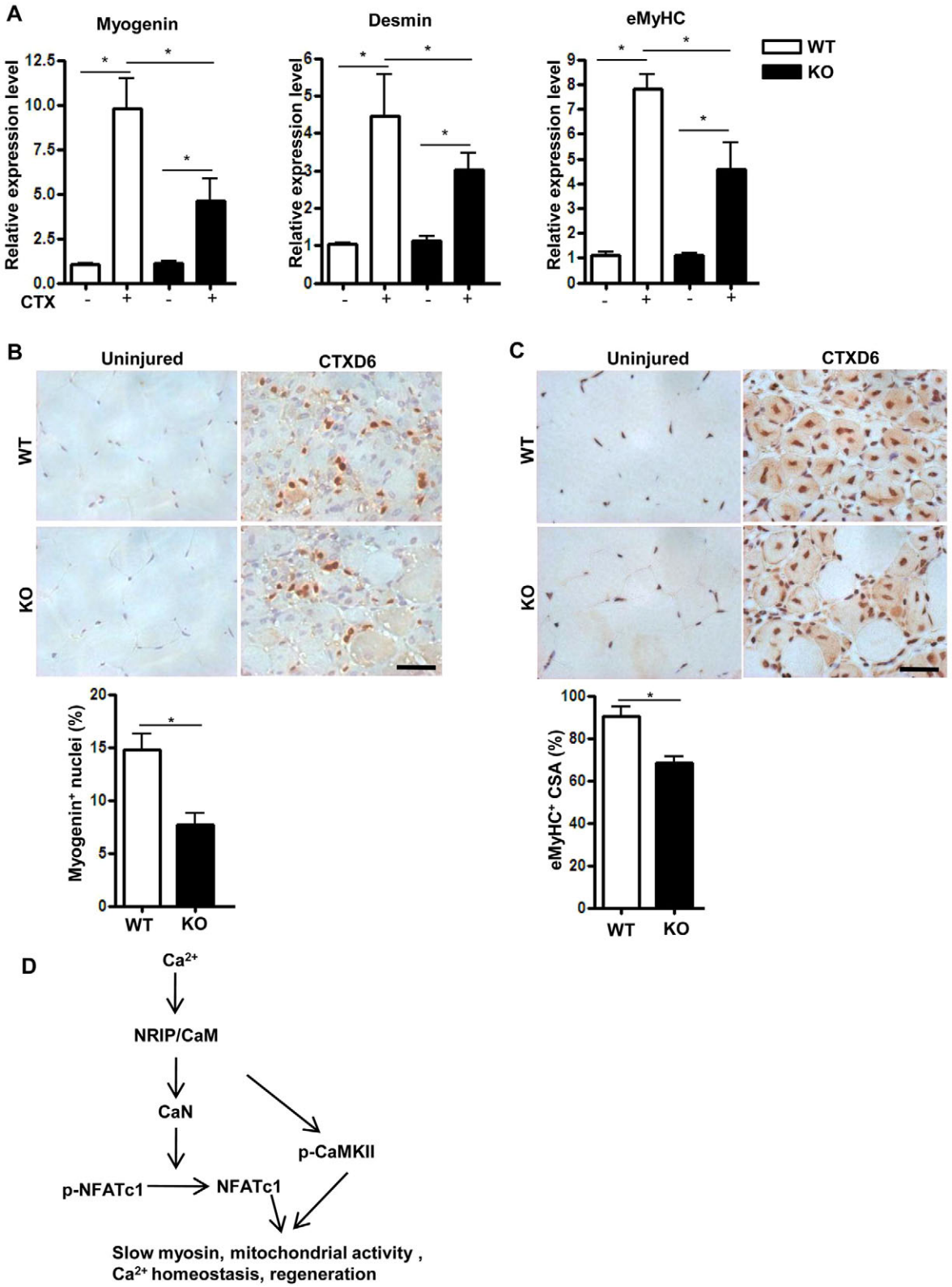

Fig. 8. NRIP regulates muscle myogenesis and myotube formation. (A) The RNA expression of regeneration markers before and after CTX-induced muscle damage at day 6 post injury. The RNA expression in the uninjured wild-type was set at 1, and the relative expression of each condition is derived from three independent experiments. (B) Myogenin expression by immunohistochemistry analysis. The cross sections of tibialis anterior muscles at day 6 after CTX injection were stained with an antibody against myogenin. Lower panel, quantification of myogenin expression. n=5. Scale bar: 100 µm. (C) eMyHC (MYH3) expression was analyzed by using immunohistochemistry at day 6 after CTX injury. Lower panel, quantification of eMyHC as described in B. CSA, cross-sectional area. Scale bar: 100 µm. (D) Working model of NRIP in the regulation of muscle contraction and regeneration. NRIP and CaM (NRIP/CaM) function downstream of Ca^{2+} to trigger the activation of CaN and CaMKII, and in turn to stimulate the expression of slow myosin genes and mitochondrial activity, to maintain Ca^{2+} homeostasis in SR storage and to promote regeneration. KO, knockout; p-, phosphorylated protein; WT, wild type. Mean±s.e.m.; *P<0.05 (Student's t-test).

Journal of Cell Science (2015) 128, 4196-4209 doi:10.1242/jcs.174441

days after injection with CTX, wild-type and knockout mice had broad myofiber degeneration and accumulations of small mononucleated cells at the site of injury (Fig. 7D, CTXD3), and there was no significant difference (Fig. 7E, day 3). However, the amount of degeneration was higher in NRIP-knockout than in wild-type mice at days 6, 12 and 21 post injury (Fig. 7E). During the process of regeneration, NRIP-knockout mice had fewer centralized nuclei, smaller myofibers and an increased amount of degenerated tissues compared with wild-type mice. Thus, NRIP deletion delays but does not completely prevent regeneration.

NRIP can induce terminal differentiation and myotube formation during muscle regeneration

In examining the role of NRIP in muscle regeneration, we found that NRIP expression was particularly increased in the nuclei of cells after muscle injury in the tibialis anterior muscles of wild-type mice (Fig. S4A). The increase in NRIP correlated with increasing amounts of paired box protein 7 (Pax7), detected by western blotting at day 3 after injury (Fig. S4B). Pax7 is a muscle satellite cell marker and reportedly can be induced by muscle damage (Shi and Garry, 2006). Therefore, the finding that NRIP expression can also be enhanced after muscle injury strengthens the hypothesis that NRIP is involved in muscle regeneration. Myogenin, desmin and embryonic MyHC (eMyHC; also known as MYH3) are the key markers of the onset of terminal differentiation and myotube formation, and are hallmarks of newly regenerated fibers (Bassel-Duby and Olson, 2006). We measured the RNA expression levels of myogenin, desmin and eMyHC at day 6 after injury and found them to be significantly reduced in NRIP-knockout mice, compared to the levels in wild-type mice, during muscle regeneration (Fig. 8A). Furthermore, the myogenin protein expression at day 6 post injury is shown in Fig. 8B, and quantification of myogenin showed significantly lower amounts in NRIP-knockout mice than in wild-type mice (Fig. 8B, lower panel). Furthermore, desmin-positive myofibers were more abundant in wild-type mice than NRIP-knockout mice at day 6 post injury (Fig. S4C). Quantification of the cross-sectional area (CSA) of desmin staining showed that wild-type mice recovered about 79% of regenerative fibers, but NRIP-knockout mice exhibited a significant reduction in their ability to recover (48%) (Fig. S4D). Moreover, quantification of embryonic MyHC expression in NRIP-knockout mice showed that there was a lower amount of this protein than in wild-type mice (Fig. 8C). Hence, NRIP contributes to skeletal muscle differentiation and myotube formation during the regeneration process. In summary, NRIP acts downstream of Ca^{2+} signaling and triggers CaN and CaMKII to regulate slow myosin gene expression, mitochondrial function, Ca^{2+} homeostasis and muscle regeneration (Fig. 8D).

DISCUSSION

In this study, we show that NRIP plays a role in muscle strength and endurance. We found that NRIP-knockout mice exhibited a loss of muscle force, susceptibility to fatigue and impairment of adaptive exercise performance (Fig. 3). NRIP was previously identified as a nuclear protein and a transcription cofactor (Tsai et al., 2005). Here, NRIP was predominantly located in the cytosol and colocalized with CaN at the Z-disk of the sarcomere (Fig. 1), consistent with a previous report that NRIP is subject to Ca^{2+}-dependent CaM binding in order to activate CaN (Chang et al., 2011). This suggests that the subcellular location of NRIP might vary in different tissues. In this study, NRIP-knockout mice showed impaired CaN-NFATc1 signaling, resulting in a reduced number of type-I slow myofibers (Fig. 4). This observation was verified in cultured myoblast C2C12 cells, which showed reduced levels of activated NFATc1 (Fig. 6). Hence, the reduction in CaN-NFAT signaling and decrease in the number of type-I slow fibers might account for the impaired contractile activity and fatigue susceptibility in NRIP-knockout muscles. Consistently, activation of the expression of oxidative fatigue-resistance slow-type fibers through CaN-NFAT signaling is well documented (Harridge, 2007; Meissner et al., 2007). For example, the activation of CaN enhances muscle resistance to fatigue in *mdx* mice (a model of Duchenne muscular dystrophy) (Frey et al., 2008; Stupka et al., 2008) and increases the number of slow-twitch muscle fibers (Naya et al., 2000). By contrast, genetic disruption of CaN leads to a significant decrease in slow-twitch and oxidative fibers (Parsons et al., 2003).

Here, NRIP is shown to have an effect on mitochondrial activity. We found that PGC1-α was expressed at lower levels in cells following depletion of NRIP, and NRIP-knockout mice displayed reduced mitochondrial activities (COX and SDH) that might account for the reduced muscle force (Fig. 4G–I). NRIP can regulate slow myosin expression; the slow-twitch fibers have a high content of mitochondria, and exhibit resistance to fatigue and high oxidative capacity (Russell et al., 2014). Hence, NRIP can control slow myosin expression in a manner that might be related to effects on mitochondrial function. Recently, growing evidence has shown that the mitochondria in skeletal muscle alter with age (Peterson et al., 2012). Aging gradually results in loss of muscle mass and muscle strength. The decline of mitochondrial function in skeletal muscle plays a key role in the aging process. Further studies to determine how NRIP regulates mitochondrial biogenesis and activities would be of value.

In addition to the Ca^{2+}-sensitive signaling protein CaN, CaMKII is also regulated by Ca^{2+}-dependent CaM binding (Rose et al., 2006) and its phosphorylation regulates Ca^{2+} release and uptake (Lanner et al., 2010; Treves et al., 2008). Here, we showed that NRIP triggered CaMKII phosphorylation (Fig. 5A), because NRIP enhances the binding affinity of CaM for CaN and CaMKII (Fig. 3E). In terms of maintaining Ca^{2+} homeostasis, our results showed that NRIP-knockout mice lack CaMKII phosphorylation and exhibit a weak caffeine-induced maximal Ca^{2+} release that resulted from the efflux of internally stored Ca^{2+} from the SR (Fig. 5). It seems that NRIP-knockout mice have reduced Ca^{2+} storage compared to wild-type mice, resulting in a defect in Ca^{2+} release from the SR into the cytosol that weakens muscle contractile strength and reduces endurance. These findings indicate that NRIP regulates the balance of Ca^{2+} storage to influence the contraction of skeletal muscle through CaMKII phosphorylation.

In this study, NRIP was shown to regulate slow myosin gene expression, mitochondrial function and Ca^{2+} storage in the SR. Activation of slow myosin genes has been reported not only to be through the CaN-NFATc1 pathway but also through CaMKII activity. The activated CaMKII acts through the phosphorylation of class-II histone deacetylases (HDACs), which lose their repressive effects as a result, allowing myocyte enhancer factor 2 (MEF2)-dependent transcriptional activation of slow myosin genes. Thus, NRIP regulation of slow myosin gene expression might be mediated through CaMKII, as well as CaN. As to the effect of NRIP on Ca^{2+} storage in the SR through CaMKII, CaN also has been reported to be associated with the L-type Ca^{2+} channel at the plasma membrane in the heart, where it activates the channel to increase Ca^{2+} influx (Heineke et al., 2010). We can infer that NRIP induces slow myosin gene expression and Ca^{2+} homeostasis through either CaN or CaMKII signaling. Moreover, in investigating the activity of NRIP in cells, a Ca^{2+} ionophore alone can increase the amount of nuclear NFATc1 (activated form) and phosphorylated CaMKII. Depletion

Journal of Cell Science (2015) 128, 4196-4209 doi:10.1242/jcs.174441

of NRIP causes the loss of nuclear NFATc1 and of phosphorylated CaMKII, and the Ca^{2+} activator cannot restore the activated NFATc1 and phosphorylated CaMKII (Fig. 6A), indicating that NRIP functions downstream of Ca^{2+} activation. This also occurred in cells that had been treated with NRIPΔIQ, which lacks the IQ domain responsible for CaM binding (Fig. 6C), further supporting the concept of NRIP-induced CaN and CaMKII signaling through CaM binding. We describe a novel scenario in which NRIP functions downstream of Ca^{2+} to trigger CaN and CaMKII activities, resulting in the induction of slow myosin, mitochondrial function and internal Ca^{2+} storage in the SR for muscle contraction (Fig. 8D).

Here, we also showed that NRIP influences the capacity for muscle regeneration (Fig. 7). After muscle injury, NRIP-knockout mice exhibited a delayed repair capacity (Fig. 7), coupled with a reduction of myogenin-, desmin- and eMHC-positive cells (Fig. 8; Fig. S4). All of these findings support the association of NRIP with myogenesis and myotube formation during regeneration. This implies that NRIP might be linked to satellite cell differentiation and might contribute to muscle regeneration. NRIP can stimulate CaN-NFAT and CaMKII, which are involved in muscle regeneration after muscle injury or degeneration (Abraham and Shaw, 2006; Michel et al., 2004). For example, CaN and/or NFAT functions are blocked by a negative regulator (myospryn) or immunosuppressive drugs (cyclosporine A), leading to the impairment of muscle regeneration (Demonbreun et al., 2010; Kielbasa et al., 2011). Moreover, CaN transgenic mice display strong regeneration of skeletal muscle fibers after injury (Demonbreun et al., 2010; Stupka et al., 2006). In addition, the CaMK pathway can be activated by treatment with insulin-like growth factor 1 (IGF1), which has been well documented to activate satellite cells and to induce terminal myogenic differentiation (Lu et al., 2000; Song et al., 2013). Thus, NRIP promotes muscle regeneration through the CaN and CaMKII signaling pathways.

We found that NRIP-knockout mice displayed normal muscle histology but that they have less muscle force and reduced Ca^{2+} storage and mitochondrial function compared with wild-type mice. After muscle injury, knockout mice exhibited delayed repair coupled with impaired myogenic capacity. This might be explained by the observation that loss of NRIP alone does not affect muscle morphology but does, nonetheless, impair muscle function. Following stress (such as an injury), the repair process needs additional events to coordinate with NRIP in order to promote muscle regeneration – including activation and proliferation of satellite cells, and myogenic differentiation. Therefore, the molecular mechanisms underlying NRIP regulation of muscle satellite cell activation and differentiation are worthy of further investigation. Moreover, in this study we used global knockout mice to demonstrate delayed repair after muscle injury. Because the NRIP deficiency occurs in all the tissues of the knockout mice, it remains to be determined whether muscle-cell-autonomous factors or other cells (macrophages or motor neurons) that lack NRIP influence the delayed repair in these mice. Current reports demonstrate that inflammatory cells, infiltrating after muscle injury, can produce growth factors, cytokines and chemokines that can activate components of regenerative mechanisms – such as myogenic factors and satellite cells for muscle repair (Urso, 2013). Now, we are in the process of generating muscle-specific NRIP-knockout mice in order to identify NRIP-mediated regeneration activity that is derived from muscle cell autonomous factors or inflammatory cells for cell cytoprotection, or whether this activity derives from other cells (such as motor neurons).

In conclusion, expression of NRIP is age dependent (Fig. 1C), and can regulate slow myosin gene expression and mitochondrial function (Fig. 4). The slow oxidative fibers and functional mitochondria are relatively resistant to the progressive myonecrosis that occurs with advancing age in Duchenne's muscular dystrophy – characterized by a lack of dystrophin – and in individuals that suffer congestive heart failure (Chin et al., 1998; Ljubicic et al., 2011; Sabbah et al., 1993); therefore, the discovery of a factor that promotes a fast-to-slow fiber switch in individuals will be important to decrease morbidity and improve quality of life. Therefore, NRIP could be a good target for future therapeutic treatment in muscular dystrophy, chronic diseases that are characterized by physical inability and/or loss of muscle mass, and ageing.

MATERIALS AND METHODS

Generation and genotyping of NRIP-knockout mice

Mouse NRIP genomic DNA (bMQ BAC clone number bMQ134h07) was obtained by screening a BAC library derived from the 129 mouse strain. This 19.2 kb mouse genomic DNA fragment was inserted into the *Not*I–*Spe*I site of pL253, in which the MC1-TK (thymidine kinase) gene served as a negative selection marker (Chen et al., 2012). The resulting construct was used as the backbone for subsequent insertion of a loxP sequence from pL452 into intron 2 and of a neo cassette with two flanking loxP sequences from pL452 into intron 1. The targeting construct contained a homologous short 5′ arm of 4.3 kb and long 3′ arm of 10.6 kb. The targeting vector was linearized through DNA digestion with *Not*I (unique site) and electroporated into embryonic stem (ES) cells, and then G418-resistant clones were selected. The G418-resistant ES cells were then transfected with the pBabe-puro-Cre plasmid for Cre-recombinase-mediated loxP recombination to delete the NRIP exon 2. Homologous recombinant clones were identified by using Southern blot analysis, injected into blastocysts of C57BL/6JNarl mice and then implanted into pseudo-pregnant foster mothers (Chen et al., 2012). The chimeric males were recognized by coat color and were mated with C57BL/6JNarl females. The germline transmission was confirmed by PCR analysis and Southern blotting from mouse genomic DNA to confirm the deletion of NRIP exon 2 in NRIP-knockout mice. The NRIP heterozygous female mice were then back-crossed to the male C57BL/6JNarl genetic background for eight successive generations.

In vitro measurement of muscle force

Mice were euthanized, and their muscles were excised and mounted vertically with silk suture (Type BG; Gould, Cleveland, OH) tied to the proximal and distal tendons. To measure isometric force, a single twitch was evoked with 1 Hz, square pulses of 5-ms duration. Fatigue was elicited by repetitive stimulation at 100 Hz for 800 ms, once every 5 s, for a total of 300 s. To measure caffeine-induced maximal muscle force, muscles were treated with 10 mM caffeine (Sigma-Aldrich) containing tyrode solution for muscle force analysis, as described above. To calculate the combination of electrical stimulation (pacing) with caffeine-induced muscle force, diaphragm muscles were stimulated with 1 Hz, square pulses of 5-ms duration for 5 min and then treated with 10 mM caffeine.

Behavioral analysis

In the rotarod test, mice were trained three times by being placed in a neutral position in the stationary 3-cm diameter cylinder of the rotarod apparatus (Singa RT-01), then at a constant rotating speed of 5 rpm for 30 s. 30-min breaks were provided between the training and test phases. In the test phase, the constant rotating speed was set at 10 rpm, and the time to falling was recorded when each mouse fell off the rod. The treadmills (Bioseb, LE8710M) had computerized systems to record the exercise time and a spike for delivering a low-intensity electric shock to the feet of the mouse when it refused to run in the treadmill. Mice started to run on a 5% slope at a speed of 5 m/min for 30 min. Thereafter, the speed was increased to 20 m/min, and the number of electrical stimulations (a constant intensity of 2 mA) was recorded within 10 min.

Journal of Cell Science (2015) 128, 4196-4209 doi:10.1242/jcs.174441

Tissue staining

Muscles were collected and fixed in 4% paraformaldehyde for tissue staining. For hematoxylin and eosin (HE) staining, paraffin-embedded sections were deparaffinized and stained with hematoxylin (ScyTek) and eosin (Surgipath). For immunohistochemistry assays, the paraffin-embedded sections were incubated with the antibody indicated (Table S2). For immunofluorescence assays, the fluorescent signal was produced by the incubation of Cy3-conjugated goat anti-mouse or AlexFluor488-conjugated goat anti-rabbit secondary antibody (Jackson Laboratory). The images were acquired with a Leica TSC SP5 confocal microscope (Leica Microsystems, Wetzlar, Germany). For Masson's trichrome staining, the deparaffinized sections were stained with Weigert's iron hematoxylin working solution (Sigma) and Biebrich Scarlet-acid Fuchsin solution (Sigma) as per the manufacturer's protocol.

COX and SDH activities

The frozen tissue sections were incubated with solution containing 80 µM cytochrome *c* and 1300 U catalase. The sections were then mounted with PERMOUNT® synthetic organic mounting medium. COX-positive fibers were visualized through brown staining. For SDH staining, sections were incubated in a solution containing sodium succinate, phosphate buffer and nitroblue tetrazoliumand. The sections were then mounted with glycerol-based mounting medium. SDH-positive fibers were visualized by purple staining. Images were acquired with a Zeiss Imager A1 microscope and an AxioCam MRM CCD camera.

Measurement of Ca^{2+} transients

Flexor digitorum brevis muscles from 4–6 week old mice were digested with type-I collagenase (6 mg/ml), single fibers were isolated and seeded on laminin-coated coverslips. Fibers were then incubated with 5 µM Fura-2 AM (Molecular Probes, Invitrogen) and immersed in imaging buffer. The coverslips were mounted in a chamber containing imaging buffer and equipped with platinum field electrodes. Ca^{2+} signals were recorded using a dual-beam excitation fluorescence photometry setup (IonOptix). Fibers were electrically stimulated with 1 Hz or loaded with 10 mM caffeine for SR Ca^{2+} determination. Cytosolic Ca^{2+} measurements were expressed as fluorescence ratio of the emission at 480 nm with reference to the excitation wavelengths of 360 and 380 nm, respectively.

Transmission electron microscopy

The euthanized mice were perfused through the left ventricle with 30 mM KCl in tyrode solution. Briefly, the soleus was harvested and quickly fixed in 0.15 M sodium cacodylate buffer containing 2% paraformaldehyde and 2% glutaraldehyde (pH 7.4). Tissues were cut longitudinally into 60-nm sections and stained with 1% osmium tetroxide, 0.8% potassium ferrocyanide for 16 h and then treated with 2% uranyl acetate, followed by dehydration in a series of ethanol and acetone. Electron micrographs were recorded using Tecnai G2 Spirit TWIN (FEI Company). The TEM images were then imported into ImageJ Program software for measurement of SR size.

Western blotting

Muscle tissues were harvested and immediately stored in liquid nitrogen. Protein extracts were prepared in tissue lysis buffer (20 mM sodium phosphate, 150 mM NaCl, 2 mM $MgCl_2$, 10 mM NaF, 0.1 mM sodium orthovanadate, 10 mM sodium pyrophosphate, 1 mM dithiothreitol, 1% NP-40, 10 µg of leupeptin per ml, 10 µg of aprotinin per ml, 10 µg of pepstatin per ml, 10 µg of *N*-tosyl-phenylalanyl chloromethyl ketone per ml). An equal amount protein was resolved on an SDS–polyacrylamide gel, transferred to a PVDF membrane and immunodetected with the antibodies indicated (Table S2).

Real-time quantitative PCR

Muscle tissues were explanted and quickly stored in RNAlater solution (Ambion). Total RNAs were isolated with TRIzol reagent (Invitrogen) and treated with DNase (RQ1, Promega) to remove genomic DNA. One microgram of RNA was reverse transcribed into cDNA for real-time quantitative PCR (RT-qPCR) analysis. The sequences of the primers are shown in supplemental materials (Table S1).

C2C12 cell culture

C2C12 cells were grown in Dulbecco's modified Eagle's medium (DMEM; Gibco) supplemented with 10% FBS. For myoblast differentiation, the growth medium was replaced with differentiation medium, which comprised DMEM supplemented with 5% horse serum, to induce myogenic differentiation. C2C12 myoblasts were grown to 80% confluence and then infected with the virus indicated for 18 h in growth medium before differentiation. At the time indicated after differentiation, the cells were fixed for immunofluorescence or harvested for western blotting. To investigate Ca^{2+}-mediated signaling, the cells were treated with A23187 (Sigma) at a concentration of 1 µM to assay CaN and CaMKII activation.

Recombinant adenovirus generation and infection

The adenovirus encoding shNRIP was constructed by inserting NRIP-targeted RNAi into pSIREN-DNR (BD Biosciences Clontech; Knockout RNAi Systems) to form pSIREN-DNR-RNAi. The pSIREN-DNR-Luc plasmid encoding an shRNA against luciferase served as a negative control. The shRNA-expressing adenovirus was generated by subcloning a functional shRNA cassette from pSIREN-DNR-RNAi into a recombinant adenovirus vector (pLP-Adeno-X-PRLS, BD Biosciences Clontech). The adenovirus encoding Flag–NRIP (named Ad-NRIP) and Flag–NRIPΔIQ (named Ad-NRIPΔIQ) was based on the AdEasy™ vector system and cloned into the shuttle vector pAdTrack-CMV backbone. All the recombinant adenoviruses were amplified in HEK293A cells and purified using an Adeno-XTM Maxi Purification kit (Clontech), following the manufacturer's instructions.

Muscle regeneration analysis

The mice were anesthetized and injected with unilateral cardiotoxin (10 mM CTX, Sigma) into the tibialis anterior muscle, the contralateral muscle was injected with PBS and served as a control. Mice were allowed to recover for 1, 3, 6, 12 and 21 days post injury. HE staining and Masson's trichrome analysis were used to measure regeneration and degeneration levels.

Statistics

All the statistical data were generated by using Prism software (GraphPad Software). Data are reported as the mean±s.e.m. All *P*-values were determined with Student's *t*-test for comparisons between two groups. A *P*-value of less than 0.05 was considered statistically significant.

Study approval

All animal experiments were reviewed and approved by the Institutional Animal Care and Use Committee (IACUC) at the College of Medicine, National Taiwan University. All experimental mice were housed in the animal center under a 12 h light–dark cycle with free access to food and water.

Acknowledgements

NRIP-knockout mice were generated by the Transgenic Mouse Core Facility in National Taiwan University Center for Genomic Medicine. The rotarod and treadmill assays were conducted in the Behavior Core Laboratory of the Neurobiology and Cognitive Science Center; the confocal image analysis at The Imaging Core at the First Core Lab; and the paraffin section preparation in the Animal Center, National Taiwan University. Transmission electron microscopy analysis was performed in the Imaging Core, Institute of Molecular Biology, Academia Sinica, Taiwan. We also thank Dr Shu-Wha Lin for advice on generating NRIP-knockout mice, Dr Pei-Yu Wang for critical discussions, Mr Po-Yuen Wu and Mr Kuan-Liang Lin for technical assistance with the generation of NRIP-knockout mice and Dr Tim J. Harrison for language editing.

Competing interests

The authors declare no competing or financial interests.

Author contributions

H.-H.C., S.-L.C. conceived and designed the experiments. H.-H.C., W.-P.C., W.-L.Y., Y.-C.H., S.-W.C., W.-M.F., I.-S.Y., T.-C.T., Y.-T.Y. performed the experiments. H.-H.C., Y.-P.T., S.-L.C. analyzed the data. S.-L.C. contributed reagents, materials and analysis tools. H.-H.C., S.-L.C. contributed to the writing of the manuscript.

Funding

This work was supported by National Science Council [grant number NSC101-2321-B-002-061, NSC102-2320-B-002-033-MY3]; the National Health Research Institute, Taiwan [grant number NHRI-EX101- 10148SI]; and National Taiwan University [grant number 10R891903].

Supplementary information

Supplementary information available online at
http://jcs.biologists.org/lookup/suppl/doi:10.1242/jcs.174441/-/DC1

References

Abraham, S. T. and Shaw, C. (2006). Increased expression of deltaCaMKII isoforms in skeletal muscle regeneration: implications in dystrophic muscle disease. *J. Cell. Biochem.* **97**, 621-632.

Bähler, M. and Rhoads, A. (2002). Calmodulin signaling via the IQ motif. *FEBS Lett.* **513**, 107-113.

Bassel-Duby, R. and Olson, E. N. (2006). Signaling pathways in skeletal muscle remodeling. *Annu. Rev. Biochem.* **75**, 19-37.

Borselli, C., Storrie, H., Benesch-Lee, F., Shvartsman, D., Cezar, C., Lichtman, J. W., Vandenburgh, H. H. and Mooney, D. J. (2010). Functional muscle regeneration with combined delivery of angiogenesis and myogenesis factors. *Proc. Natl. Acad. Sci. USA* **107**, 3287-3292.

Calabria, E., Ciciliot, S., Moretti, I., Garcia, M., Picard, A., Dyar, K. A., Pallafacchina, G., Tothova, J., Schiaffino, S. and Murgia, M. (2009). NFAT isoforms control activity-dependent muscle fiber type specification. *Proc. Natl. Acad. Sci. USA* **106**, 13335-13340.

Chang, S.-W., Tsao, Y.-P., Lin, C.-Y. and Chen, S.-L. (2011). NRIP, a novel calmodulin binding protein, activates calcineurin to dephosphorylate human papillomavirus E2 protein. *J. Virol.* **85**, 6750-6763.

Chen, P.-H., Tsao, Y.-P., Wang, C.-C. and Chen, S.-L. (2008). Nuclear receptor interaction protein, a coactivator of androgen receptors (AR), is regulated by AR and Sp1 to feed forward and activate its own gene expression through AR protein stability. *Nucleic Acids Res.* **36**, 51-66.

Chen, C.-Y., Tsai, M.-S., Lin, C.-Y., Yu, I.-S., Chen, Y.-T., Lin, S.-R., Juan, L.-W., Chen, Y.-T., Hsu, H.-M., Lee, L.-J. et al. (2012). Rescue of the genetically engineered Cul4b mutant mouse as a potential model for human X-linked mental retardation. *Hum. Mol. Genet.* **21**, 4270-4285.

Cheung, C.-L., Chan, B. Y. Y., Chan, V., Ikegawa, S., Kou, I., Ngai, H., Smith, D., Luk, K. D. K., Huang, Q.-Y., Mori, S. et al. (2009). Pre-B-cell leukemia homeobox 1 (PBX1) shows functional and possible genetic association with bone mineral density variation. *Hum. Mol. Genet.* **18**, 679-687.

Chin, E. R., Olson, E. N., Richardson, J. A., Yang, Q., Humphries, C., Shelton, J. M., Wu, H., Zhu, W., Bassel-Duby, R. and Williams, R. S. (1998). A calcineurin-dependent transcriptional pathway controls skeletal muscle fiber type. *Genes Dev.* **12**, 2499-2509.

Demonbreun, A. R., Lapidos, K. A., Heretis, K., Levin, S., Dale, R., Pytel, P., Svensson, E. C. and McNally, E. M. (2010). Myoferlin regulation by NFAT in muscle injury, regeneration and repair. *J. Cell Sci.* **123**, 2413-2422.

Ehret, G. B., O'Connor, A. A., Weder, A., Cooper, R. S. and Chakravarti, A. (2009). Follow-up of a major linkage peak on chromosome 1 reveals suggestive QTLs associated with essential hypertension: GenNet study. *Eur. J. Hum. Genet.* **17**, 1650-1657.

Frey, N. and Olson, E. N. (2002). Calsarcin-3, a novel skeletal muscle-specific member of the calsarcin family, interacts with multiple Z-disc proteins. *J. Biol. Chem.* **277**, 13998-14004.

Frey, N., Richardson, J. A. and Olson, E. N. (2000). Calsarcins, a novel family of sarcomeric calcineurin-binding proteins. *Proc. Natl. Acad. Sci. USA* **97**, 14632-14637.

Frey, N., Frank, D., Lippl, S., Kuhn, C., Kögler, H., Barrientos, T., Rohr, C., Will, R., Müller, O. J., Weiler, H. et al. (2008). Calsarcin-2 deficiency increases exercise capacity in mice through calcineurin/NFAT activation. *J. Clin. Invest.* **118**, 3598-3608.

Garcia-Roves, P. M., Huss, J. and Holloszy, J. O. (2006). Role of calcineurin in exercise-induced mitochondrial biogenesis. *Am. J. Physiol. Endocrinol. Metab.* **290**, E1172-E1179.

Gonzalez, D. R., Beigi, F., Treuer, A. V. and Hare, J. M. (2007). Deficient ryanodine receptor S-nitrosylation increases sarcoplasmic reticulum calcium leak and arrhythmogenesis in cardiomyocytes. *Proc. Natl. Acad. Sci. USA* **104**, 20612-20617.

Harridge, S. D. R. (2007). Plasticity of human skeletal muscle: gene expression to in vivo function. *Exp. Physiol.* **92**, 783-797.

Heineke, J., Auger-Messier, M., Correll, R. N., Xu, J., Benard, M. J., Yuan, W., Drexler, H., Parise, L. V. and Molkentin, J. D. (2010). CIB1 is a regulator of pathological cardiac hypertrophy. *Nat. Med.* **16**, 872-879.

Kielbasa, O. M., Reynolds, J. G., Wu, C.-L., Snyder, C. M., Cho, M. Y., Weiler, H., Kandarian, S. and Naya, F. J. (2011). Myospryn is a calcineurin-interacting protein that negatively modulates slow-fiber-type transformation and skeletal muscle regeneration. *FASEB J.* **25**, 2276-2286.

Lanner, J. T., Georgiou, D. K., Joshi, A. D. and Hamilton, S. L. (2010). Ryanodine receptors: structure, expression, molecular details, and function in calcium release. *Cold Spring Harb. Perspect. Biol.* **2**, a003996.

Ljubicic, V., Miura, P., Burt, M., Boudreault, L., Khogali, S., Lunde, J. A., Renaud, J.-M. and Jasmin, B. J. (2011). Chronic AMPK activation evokes the slow, oxidative myogenic program and triggers beneficial adaptations in mdx mouse skeletal muscle. *Hum. Mol. Genet.* **20**, 3478-3493.

Lu, J., McKinsey, T. A., Zhang, C.-L. and Olson, E. N. (2000). Regulation of skeletal myogenesis by association of the MEF2 transcription factor with class II histone deacetylases. *Mol. Cell* **6**, 233-244.

MacLean, H. E., Chiu, W. S. M., Notini, A. J., Axell, A.-M., Davey, R. A., McManus, J. F., Ma, C., Plant, D. R., Lynch, G. S. and Zajac, J. D. (2008). Impaired skeletal muscle development and function in male, but not female, genomic androgen receptor knockout mice. *FASEB J.* **22**, 2676-2689.

Martyn, J. A. J., White, D. A., Gronert, G. A., Jaffe, R. S. and Ward, J. M. (1992). Up-and-down regulation of skeletal muscle acetylcholine receptors effects on neuromuscular blockers. *Anesthesiology* **76**, 822-843.

McKinsey, T. A., Zhang, C. L. and Olson, E. N. (2000). Activation of the myocyte enhancer factor-2 transcription factor by calcium/calmodulin-dependent protein kinase-stimulated binding of 14-3-3 to histone deacetylase 5. *Proc. Natl. Acad. Sci. USA* **97**, 14400-14405.

Meissner, J. D., Umeda, P. K., Chang, K.-C., Gros, G. and Scheibe, R. J. (2007). Activation of the beta myosin heavy chain promoter by MEF-2D, MyoD, p300, and the calcineurin/NFATc1 pathway. *J. Cell Physiol.* **211**, 138-148.

Michel, R. N., Dunn, S. E. and Chin, E. R. (2004). Calcineurin and skeletal muscle growth. *Proc. Nutr. Soc.* **63**, 341-349.

Mokalled, M. H., Johnson, A. N., Creemers, E. E. and Olson, E. N. (2012). MASTR directs MyoD-dependent satellite cell differentiation during skeletal muscle regeneration. *Genes Dev.* **26**, 190-202.

Naya, F. J., Mercer, B., Shelton, J., Richardson, J. A., Williams, R. S. and Olson, E. N. (2000). Stimulation of slow skeletal muscle fiber gene expression by calcineurin in vivo. *J. Biol. Chem.* **275**, 4545-4548.

Ophoff, J., Van Proeyen, K., Callewaert, F., De Gendt, K., De Bock, K., Vanden Bosch, A., Verhoeven, G., Hespel, P. and Vanderschueren, D. (2009). Androgen signaling in myocytes contributes to the maintenance of muscle mass and fiber type regulation but not to muscle strength or fatigue. *Endocrinology* **150**, 3558-3566.

Parsons, S. A., Wilkins, B. J., Bueno, O. F. and Molkentin, J. D. (2003). Altered skeletal muscle phenotypes in calcineurin Aalpha and Abeta gene-targeted mice. *Mol. Cell. Biol.* **23**, 4331-4343.

Peterson, C. M., Johannsen, D. L. and Ravussin, E. (2012). Skeletal muscle mitochondria and aging: a review. *J. Aging Res.* **2012**, 194821.

Rose, A. J., Kiens, B. and Richter, E. A. (2006). Ca2+-calmodulin-dependent protein kinase expression and signalling in skeletal muscle during exercise. *J. Physiol.* **574**, 889-903.

Russell, A. P., Foletta, V. C., Snow, R. J. and Wadley, G. D. (2014). Skeletal muscle mitochondria: a major player in exercise, health and disease. *Biochim. Biophys. Acta* **1840**, 1276-1284.

Sabbah, H. N., Hansen-Smith, F., Sharov, V. G., Kono, T., Lesch, M., Gengo, P. J., Steffen, R. P., Levine, T. B. and Goldstein, S. (1993). Decreased proportion of type I myofibers in skeletal muscle of dogs with chronic heart failure. *Circulation* **87**, 1729-1737.

Shi, X. and Garry, D. J. (2006). Muscle stem cells in development, regeneration, and disease. *Genes Dev.* **20**, 1692-1708.

Shi, Y., Li, Z., Xu, Q., Wang, T., Li, T., Shen, J., Zhang, F., Chen, J., Zhou, G., Ji, W. et al. (2011). Common variants on 8p12 and 1q24.2 confer risk of schizophrenia. *Nat. Genet.* **43**, 1224-1227.

Song, Y.-H., Song, J. L., Delafontaine, P. and Godard, M. P. (2013). The therapeutic potential of IGF-I in skeletal muscle repair. *Trends Endocrinol. Metab.* **24**, 310-319.

Stupka, N., Plant, D. R., Schertzer, J. D., Emerson, T. M., Bassel-Duby, R., Olson, E. N. and Lynch, G. S. (2006). Activated calcineurin ameliorates contraction-induced injury to skeletal muscles of mdx dystrophic mice. *J. Physiol.* **575**, 645-656.

Stupka, N., Schertzer, J. D., Bassel-Duby, R., Olson, E. N. and Lynch, G. S. (2008). Stimulation of calcineurin Aalpha activity attenuates muscle pathophysiology in mdx dystrophic mice. *Am. J. Physiol. Regul. Integr. Comp. Physiol.* **294**, R983-R992.

Treves, S., Jungbluth, H., Muntoni, F. and Zorzato, F. (2008). Congenital muscle disorders with cores: the ryanodine receptor calcium channel paradigm. *Curr. Opin. Pharmacol.* **8**, 319-326.

Tsai, T.-C., Lee, Y.-L., Hsiao, W.-C., Tsao, Y.-P. and Chen, S.-L. (2005). NRIP, a novel nuclear receptor interaction protein, enhances the transcriptional activity of nuclear receptors. *J. Biol. Chem.* **280**, 20000-20009.

Urso, M. L. (2013). Anti-inflammatory interventions and skeletal muscle injury: benefit or detriment? *J. Appl. Physiol.* **115**, 920-928.

Zhang, Y., Ye, J., Chen, D., Zhao, X., Xiao, X., Tai, S., Yang, W. and Zhu, D. (2006). Differential expression profiling between the relative normal and dystrophic muscle tissues from the same LGMD patient. *J. Transl. Med.* **4**, 53.

Supplementary Figures

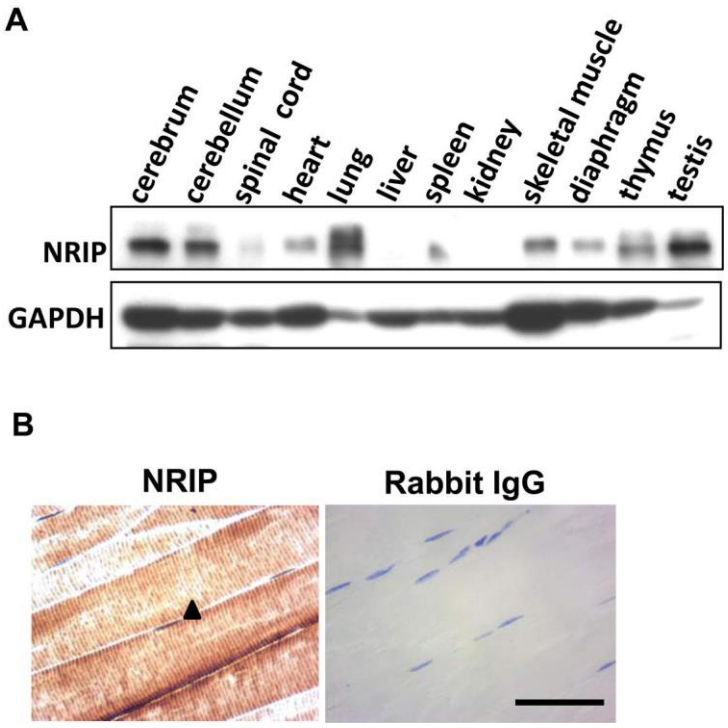

Fig. S1. (A) The distribution of NRIP protein in various tissues in 8 week old male mice analyzed by western blotting. (B) The expression of NRIP by IHC. The diaphragm muscles from WT mice were dissected longitudinally. NRIP: staining with primary NRIP antibody. Rabbit IgG: without primary NRIP antibody instead of rabbit IgG. Arrowhead: nucleus. Scale bar, 50 μm.

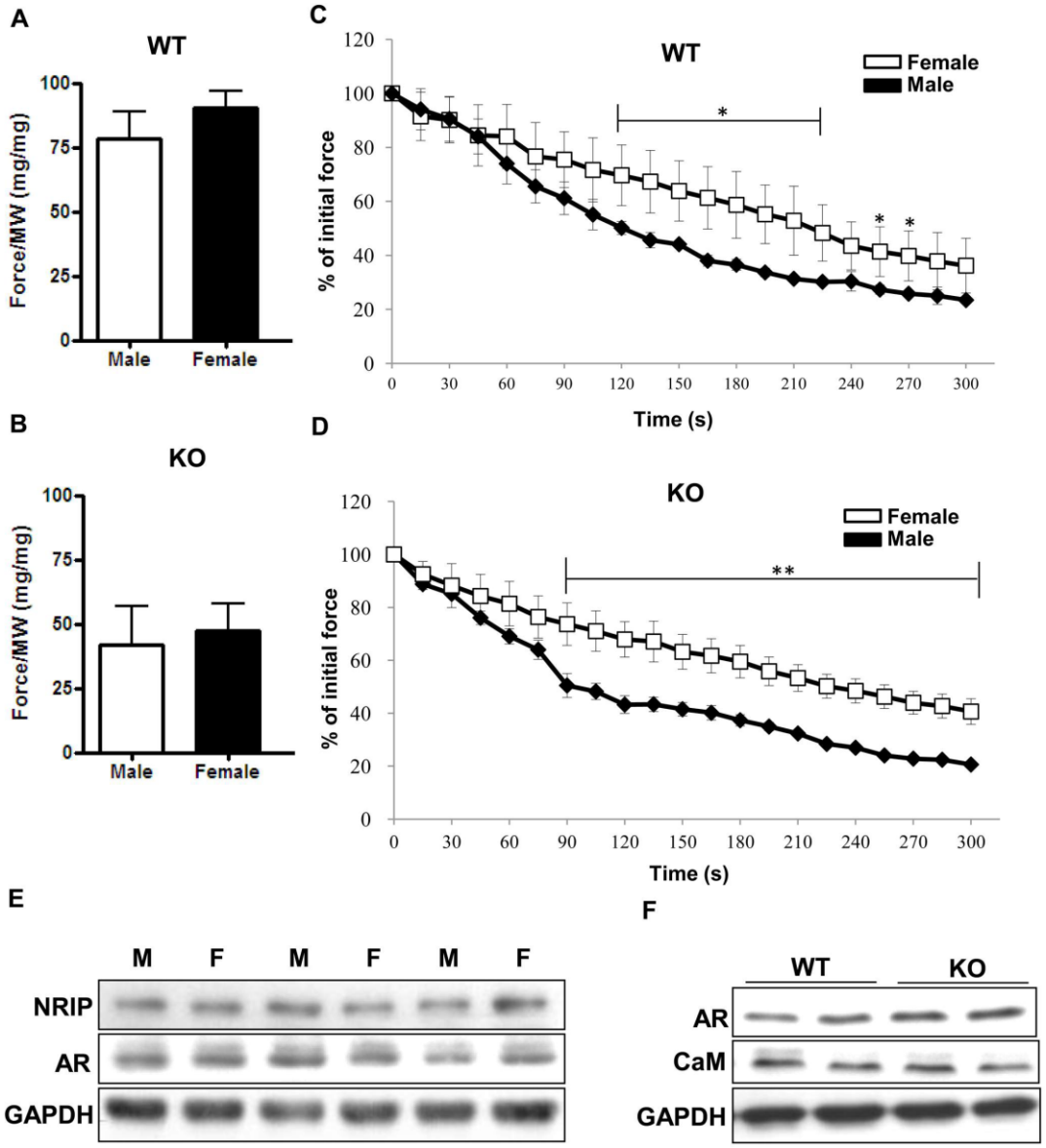

Fig. S2. Gender effect on isometric twitch force and muscle fatigue resistance. The data shown in Fig. 3A-3D were analyzed further according to sex. (A) The isometric twitch force was analyzed in WT males and females. (B) The isometric twitch force in male and female NRIP KO mice. (C) Muscle fatigue resistance in male and female WT mice. (D) The muscle fatigue resistance in male and female NRIP KO mice. The data shown in panel A-D are shown as mean ± s.e.m. and analyzed by student's *t* test**.** n=6. (E) The expression of AR and NRIP in soleus tissues from males and females by western blot. (F) The expression of AR and CaM in soleus tissues from WT and NRIP KO by western blot.

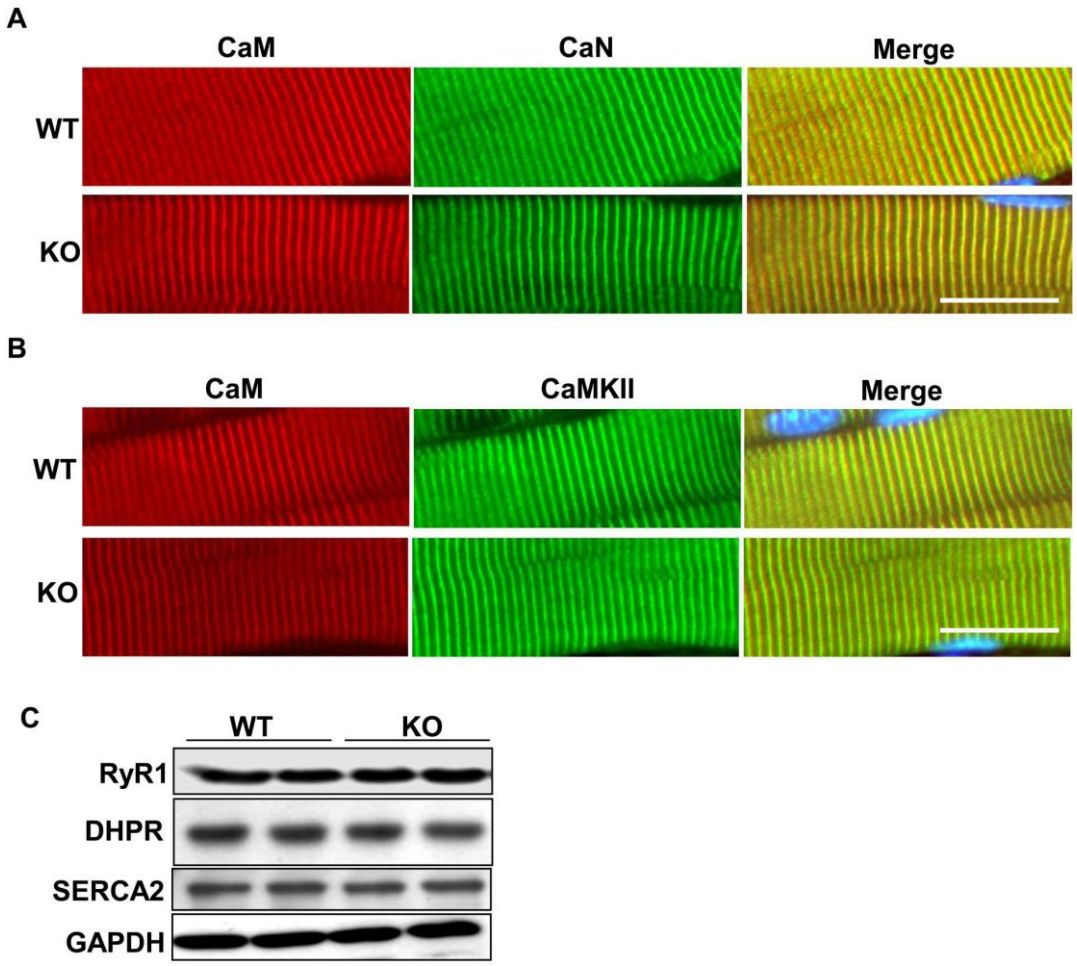

Fig. S3. The location and expression of calcium related factors in muscle tissues.

(A) The colocalization of CaM and CaN in WT and NRIP KO muscles. Gastrocnemius muscle frozen sections were stained with CaM and CaN antibody and analyzed by confocal microscopy. (B) The colocalization of CaM and CaMKII in WT and NRIP KO muscles. (C) The expression of RyR1, SERCA and DHPR in gastrocnemius tissues from WT and NRIP KO by western blot.

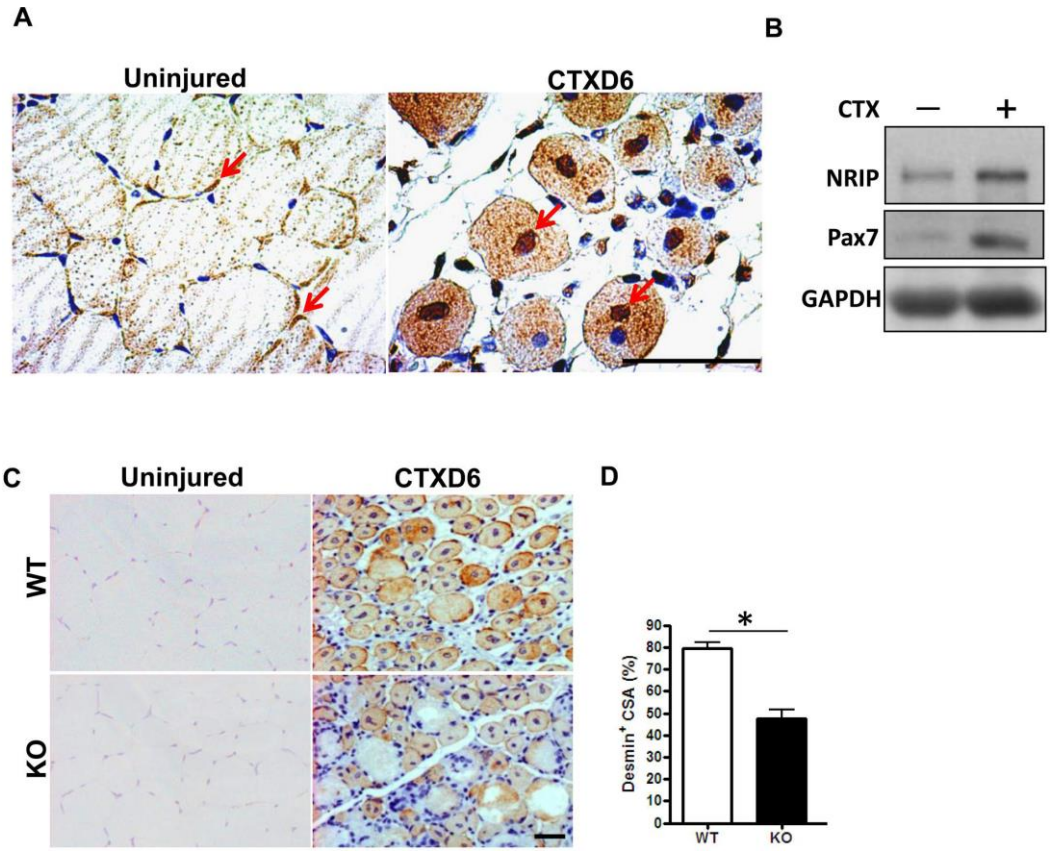

Fig. S4. NRIP expression is enhanced after muscle injury and correlates with desmin. (A) IHC assay of NRIP in CTX-injured muscle. The TA muscle tissues at day 6 post-injury were analyzed by IHC for NRIP protein expression. Hematoxylin was used to counter-stain the nucleus. 400x magnification. Arrow: NRIP nuclear staining. Scale bar, 50 μm. (B) NRIP and Pax7 increase after muscle damage, western blotting at day 3 after CTX treatment. (C) Desmin expression by IHC at day 6 post-injury. Desmin is a regeneration marker detected by brown staining. (D) Quantitation by Image-J Program in five sections per mouse and six mice of each genotype. Data are presented as mean ± s.e.m. and analyzed by student's *t* test. Scale bar, 50 μm.

Table S1. Primer sequences.

Real-time qPCR	
Gene Name	Primer Sequences
Myh4	forward 5’-CAACCCATATGACTTGCTTACGT reverse 5’-TCCCAGGATATCAACAGCAGTGT
Myh1	forward 5’-GCCGGATCTAATCGAAATGC reverse 5’-CTCCCCCTGACTGACAAAGG
Myh2	forward 5’-CAACCTCAAAGAGCGTTATGCA reverse 5’-AGGGTTGACGGTGACACAGAA
Myh7	forward 5’-CCTCCTCACATCTTCTCCATCTCT reverse 5’-TGGACTGATTCTCCCGATCTG
MCIP1.4	forward 5’- TTGTGTGGCAAACGATGATGTCTTCA reverse 5’- TGTGAACTTCCTATGTGTAAAGTC
NRIP	forward 5’- TGGAAGAGCTGGATACTTTGAACA reverse 5’- AGTTGCGGTGGCCCTTATAAA
Rpl7	forward 5’-GAAGCTCATCTATGAGAAGGC reverse 5’-AAGACGA AGGAGCTGCAGAAC
Myogenin	forward 5'-GCTGTATGAAACATCCCCCTA reverse 5'-CGCTGTGGGAGTTGCATT
Desmin	forward 5'-TACACCT GCGAGATTGATGC reverse 5'-ACATCCAA GGCCATCTTCAC
PGC-1α	forward 5'-AAACTTGCTAGCGGTCCTCA
	reverse 5'-TGGCTGGTGCCAGTAAGAG
Genotyping	
Primer Name	Primer Sequences
AU	5'-AGGTAGATTTCTGAGTTTGAGG
KU	5'-GCTTACTTTCATTTATCCCTCTTTG
XD	5'-GACATTCTTATCAGCTACACTAG
Southern blot	
Primer Name	Primer Sequences
Probe	forward 5'- GAGAAAATGGGGGAGTTGGT reverse 5'-TCTGGGAGGCTGTAGTTGCT

Table S2. Antibodies.

Western blotting			
Antibody Name	Company	Cat No.	Dilution
NRIP	Novus	A302-434A	1/2000
NFATc1	Abcam	ab25916	1/1000
CaMKII	cell signaling	3362S	1/1000
p-CaMKII	cell signaling	3361S	1/1000
Slow myosin	Abcam	ab11083	1/2000
Myogenin	SantaCruz	sc-12732	1/1000
Total myosin	Abcam	ab124205	1/1000
Flag	Abcam	ab1162	1/2000
DHPR	Abcam	ab2864	1/1000
RyR	Abcam	ab2868	1/500
SERCA2	Abcam	ab2861	1/2000
CaM	Abcam	ab45689	1/2000
GAPDH	AbFrontier	LF-PA0212	1/10000
Tissue stain			
Antibody Name	Company	Cat No.	Dilution
NRIP	Gentex	GTX105954	1/200
Slow myosin	Abcam	ab11083	1/500
NFATc1	Abcam	ab25916	1/100
Myogenin	SantaCruz	sc-12732	1/100
Desmin	Sigma	D8281	1/200
Embryonic MyHC	Abcam	ab49457	1/50
Pax7	Sigma	SAB1404168	1/100
Calcineurin	BD Bioscience	610259	1/100
CaM	Abcam	ab45689	1/100
CaMKII	cell signaling	3362S	1/100